An Investigation on Lateral String Stability in Homogeneous Vehicle Platoons

Anurodh Mishra

DC 2016.008

Internship Report

Supervisor: Prof. Dr. H. Nijmeijer (Eindhoven University of Technology)
Coaches: Dr. Ir. Igo Besselink (Eindhoven University of Technology)
Ir. Menno Beenakkers (DAF Trucks N.V.)

Eindhoven University of Technology
Department of Mechanical Engineering
Dynamics & Control

Eindhoven, November 13, 2015

This page is intentionally left blank!

Preface

This report is a part of my internship at DAF Trucks N.V., Eindhoven, the Netherlands. The report constitutes of two sections. The first section is dedicated to simulation of ADAS systems developed by DAF Trucks N.V. on a physics based simulation platform called PreScan. Being a manufacturer of commercial vehicles in Europe, DAF Trucks N.V. is taking steps towards the development of autonomous vehicles to provide greater benefit to its customer base. A number of ADAS functions are being developed at DAF in collaboration with Eindhoven University of Technology. This internship project contributes to ADAS projects at DAF, specifically Auto Docking and Blind Spot Detection, with the aim of evaluating capabilities of PreScan software through simulation of these ADAS functions. This also lays some ground work for the second part of the project.

The second part of the report is dedicated to the investigation of string stability for lateral control based on linearized bicycle model for truck-trailer combination. Analogous to the much researched longitudinal string stability, the condition for achieving lateral string stability is derived to enable design of controllers capable of forming string stable platoon systems.

Finally conclusions are drawn based upon the results achieved in an attempt to provide insight into controller design for such applications. Recommendations for future development are also made.

Anurodh Mishra
November 13, 2015

Acknowledgements

My time at DAF has been more than a learning experience. It has not only given me a direction for my master studies but also has introduced me to the corporate culture in Netherlands. I would like to take this time to show my gratitude to the people who have made this possible.

First I would like to thank DAF management for providing me the opportunity to intern at this prestigious company. I would also like to show my gratitude to the project manager, Albert van der Knaap, for the encouragement to take this project forward. A special thanks to my mentor - Menno Beenakkers for his support and guidance. He has been encouraging as well as patient during my time at DAF. I also had the opportunity to learn practical aspects of project management from him which helped me provide direction to my work. I would also like to thanks Rudolf Huisman, Johan Broeders, Thierry Kabos, Ashwin Dayal, Ivan Surovtcev, Victor Raue and Rene Vugts for providing me guidance during the project. A special thanks to Dino Sepac and J.A. Colins for making my time at DAF enjoyable.

Finally I would like to thank Dr. I.J.M. Besselink and Professor Dr. Henk Nijmeijer for their support and guidance throughout the project.

Anurodh Mishra
November 13, 2015

List of Symbols and Abbreviations

List of Symbols

u	longitudinal velocity [m/s]
m_1	mass of tractor [kg]
m_2	mass of trailer [kg]
y_1	lateral distance traversed by tractor in the body fixed frame [m]
y_2	lateral distance traversed by trailer in the body fixed frame [m]
ϕ_1	orientation of the tractor [rad]
ϕ_2	orientation of the trailer [rad]
F_{yi}	force at the i_{th} axle [N]
F_{hitch}	force at the hitching/coupling position [N]
C_i	lumped cornering stiffness at the i_{th} axle [N/rad]
α_i	wheel slip angle at the i_th axle [rad]
θ	trailer articulation angle [rad]
I_{zz1}	moment of inertia in z (vertical) direction for tractor [kg-m^2]
I_{zz2}	moment of inertia in z (vertical) direction for trailer [kg-m^2]
δ	steering input at wheel [rad]
v	lateral velocity of the tractor center of gravity [m/s]
v_{ref}	reference lateral velocity of the tractor center of gravity for the receding vehicle [m/s]
ϕ_{ref}	reference orientation of the tractor for the preceding vehicle [m/s]
y_L	lateral offset of the preceding vehicle w.r.t. vehicle centerline [m]
τ	delay time for feedforward signal [s]
L_f,d	following distance or inter-vehicular distance [m]
R	radius of curve [m]
K_c	second order compensation fucntion [-]
K_{yL}	lateral offset controller [-]
K_v	lateral velocity controller [-]
K_ϕ	yaw rate controller [-]
F	feedforward filter [-]
D	delay function [-]
K	feedback controller [-]
G	plant model [-]
q_i	generalized states for the vehicle model of i_{th} vehcile in platoon [-]
u_i	generalized input for the vehicle model of i_{th} vehcile in platoon [-]
e_i	generalized error for the vehicle model of i_{th} vehcile in platoon [-]
ω	frequency [rad/s]
f_{dip}	frequency at which dip occurs [Hz]

Abbreviations

ITS	Intelligent Transportation System
ADAS	Advance Driver Assistance System
V2V	Vehicle to Vehicle
V2I	Vehicle to Infrastructure
LIDAR	Light Detection and Ranging
DSRC	Dedicated Short Range Communication
CAD	Computer Aided Design
OEM	Original Equipment Manufacturer
BSD	Blind Spot Detection
ACC	Adaptive Cruise Control
CACC	Cooperative Adaptive Cruise Control
ALKAS	Active Lane Keeping Assist System

Contents

1. Introduction

Safety and efficiency are the keywords for the future of the automotive sector. Increasing number of accidents caused by humor error and ever growing presence of vehicles on road has put immense pressure on the existing infrastructure and put forward a demand for vehicles which are not only safe but also deal with the enormous issue of traffic management. Infrastructure is reaching its limits and to build more requires huge amount of money and energy. An alternative to this is to increase the efficiency of existing road network by supplementing vehicles with innovative technologies and usher in a new era of so-called intelligent vehicles or **Intelligent Transportation System (ITS)**.

The research on intelligent vehicles has been a very active area in recent years and has seen many companies/OEMs (Original Equipment Manufacturers) invest in technology to help make the daily experience of its customers safer and more efficient. One way to do this is to reduce the element of uncertainty introduced by human drivers by developing support systems popularly known as **Advance Driver Assistance Systems (ADAS)**. Such systems have been the focus area for the automotive sector in the recent past. The next step may be to replace human drivers with an intelligent autonomous system capable of driving like human beings but without their limitations. Such an autonomous vehicle would be capable of communicating with other similar intelligent vehicles and infrastructure to not only deliver a safer means of transportation but also utilize the current road network to its fullest capacity. One way to do this is through vehicle platooning, discussed later, which is gradually gaining popularity in the automotive industry.

However, there are many challenges to be overcome to fulfill such an endeavor. The existing infrastructure may need to be modified to accommodate the technology that would be an integral part of such autonomous vehicles. However it is very expensive economically and hence the focus has been to develop such systems within the confines of existing infrastructure. Provisions and support from the government is required to make such vehicles attractive to the common public. Additional support services need to be developed that provide a solid platform for such vehicles to be economically viable for both personal and commercial use. Especially in commercial segment, the industry has begun to see the advantages of such intelligent transportation systems and has invested heavily in developing ADAS systems.

In this report, two crucial components of vehicle automation has been discussed. Chapter 2 discuses the ever increasing complexity in vehicles due to the introduction of ADAS functions and the advantages that can be derived from software packages, like PreScan, which provide the ability to validate controller design in a virtual environment. Chapter 3 deals with the stability analysis in a vehicle platoon and discusses the notion of string stability in lateral direction.

2. ADAS Implementation on PreScan

2.1 Introduction

Safety concerns over the past decade has brought advancements in driver assistance systems. These systems are generally categorized as **Advanced Driver Assistance Systems** and are primarily aimed at

1. improving safety by minimizing human induced errors
2. improving the driver experience
3. improving vehicle performance
4. improving economy, thus, cost benefits

The benefits for developing such systems are shared by both the manufacturer, in terms of greater sales, as well as the customer, in terms of a richer and safer experience. As a result almost all major companies in the automotive sector are working on developing ADAS functions and thus, there are numerous functions existing in the market which are bound to grow.

2.2 ADAS Functions

Most ADAS applications involve use of large quantities of data from different sensors such as radar, lidar, ultrasonic, laser and image based systems which need to be processed and validated before being used for control applications. Sensor technology has grown over the years to keep up with the requirements of the industry and has grown into a complex system. The validation and testing of such a complex system is both expensive and time consuming. This has seen a rise in number of simulation software packages that enable the companies developing ADAS functions to test their control design in a virtual environment saving development time and cost. One such tool is PreScan from TASS International, which enables simulation of appropriate scenarios to test ADAS functions together with in-built sensor models. The aim of the project is to simulate two ADAS functions, namely Auto Docking and Blind Spot Detection, and evaluate PreScan as an ADAS development tool.

In the context of this report, the subsequent sub-sections provide the details of the two ADAS functions - Auto Docking and Blind Spot Detection.

2.2.1 Auto Docking

Auto Docking is the autonomous maneuvering of a commercial tractor-trailer combination vehicle from a given initial position to final docking point reserved for unloading of cargo in a controlled docking environment with no interference from other moving vehicles.

This project was performed by Thierry Kabos, ASD stduent, Eindhoven University of Technology for the Vehicle Control (VC) department in Advanced Technology (AT) group at DAF. With several

components to the project, a number of other departments from DAF were also involved. [3]

The docking station is fitted with LIDAR, which tracks the position of the vehicle combination and communicates the position over wireless communication to the vehicle itself. The LIDAR is located in a horizontal plane parallel to ground at a height of 2 m. The vehicle speeds involved are kept very low at around 1 m/s for obvious safety reasons. A path based controller was already designed to establish the objective. The truck model is a kinematic model with steering angle at wheel δ as the input and the trailer states and articulation angle as the outputs. The vector diagram of the kinematic model is shown in figure 2.1.

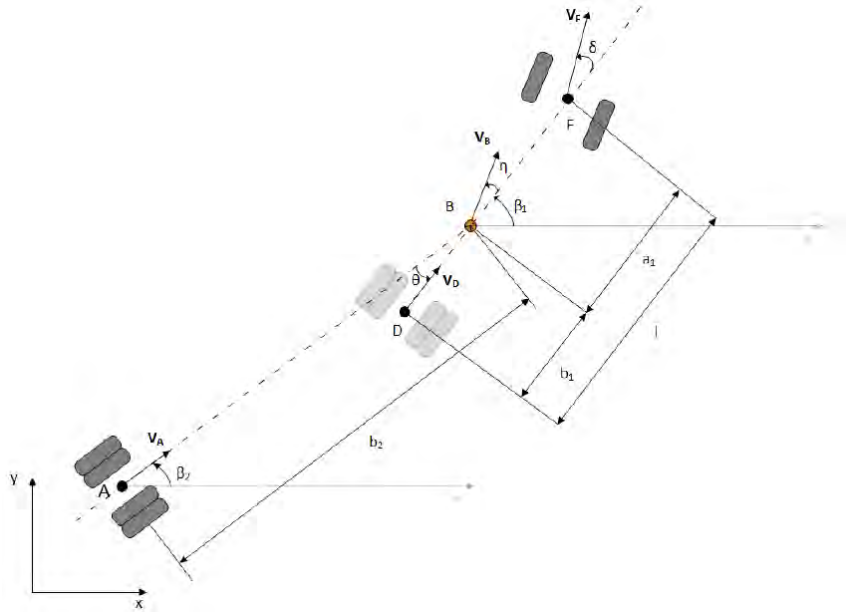

Figure 2.1: Kinematic model of tractor-trailer combination [3]

Assuming no slip conditions and a constant longitudinal velocity, u, for the tractor, the kinematic model shown in figure 2.1 can be represented by a nonlinear state space model. The notation used for the nonlinear state space model can be found in the appendix A.1.

$$\begin{pmatrix} \dot{x}_A \\ \dot{y}_A \\ \dot{\beta}_1 \\ \dot{\theta} \end{pmatrix} = u \cdot \begin{pmatrix} cos(\theta)cos(\beta_1-\theta) - \frac{b_1}{l}tan(\delta)sin(\theta)cos(\beta_1-\theta) \\ cos(\theta)sin(\beta_1-\theta) - \frac{b_1}{l}tan(\delta)sin(\theta)sin(\beta_1-\theta) \\ \frac{1}{l}tan(\delta) \\ \left(\frac{1}{l} - \frac{b_1}{b_2 l}cos(\theta)\right)tan(\delta) - \frac{1}{b_2}sin(\theta) \end{pmatrix}$$

where the articulation angle equals $\theta = \beta_1 - \beta_2$ from geometry. The reader is advised to refer to [11] for a detailed derivation of the kinematic model.

The concept of path tracking with the look-ahead distance based upon a linearized model around a reference trajectory is shown as a diagram in figure 2.2. The figure shows the trailer as a bicycle model with the articulation angle θ as the steer input. The reference path is required to be tracked by the center of the rear axle of the trailer denoted by point **A**. The tangent to the reference path corresponding to the look-ahead point gives the reference orientation of the trailer at that point,

assuming no-slip conditions. The model is linearized around the reference path to yield the error states - lateral offset, d, at a look-ahead point at a distance, L, and error in orientation, $\beta_{ref} - \beta_2 = \xi_\beta$, at the same point where, as already explained, β_{ref} is the tangent at the point **Z** to the reference path.

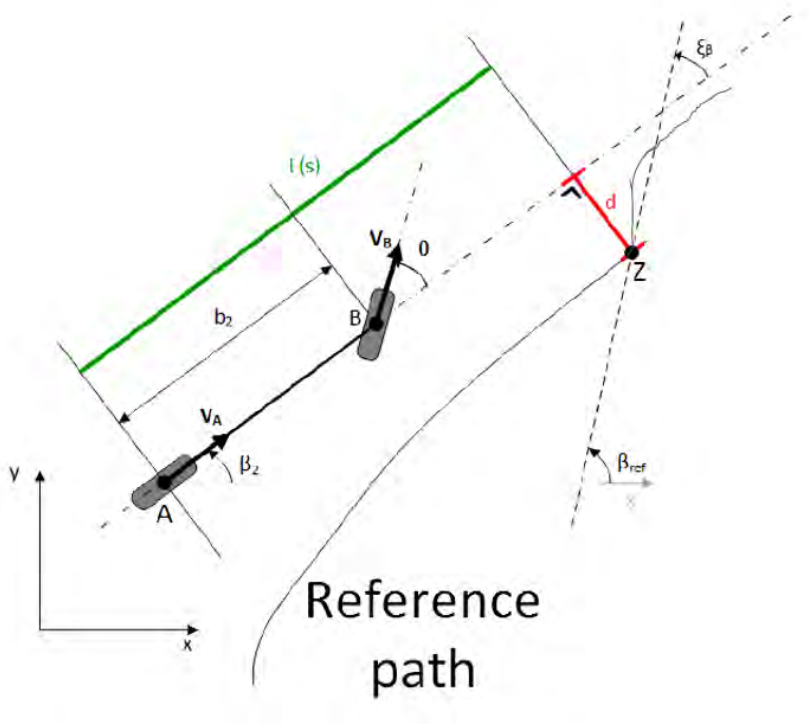

Figure 2.2: Path tracking with look-ahead distance - Auto Docking [6]

The reference path to be tracked by the rear axle of the trailer is constructed trying to mimic the path a human driver would take for the given application of docking, keeping in mind the feasibility and smoothness of the path. Such a reference trajectory is shown in figure 2.3(a). The path is derived from standpoint of practicality rather than optimality and hence is constructed using straight lines and constant radius curves to facilitate the analysis. The cascade control scheme for the control design of the system is depicted in figure 2.3(b). It has two controllers C_1 and C_2. The global position, x_{ref} and y_{ref}, and orientation, β_{ref}, for the reference path are fed to the vehicle model which outputs the error states d i.e. the lateral offset from the reference path at the look-ahead point and ξ_β i.e. the error in orientation of the trailer w.r.t. the reference orientation. This serves as the input to controller C_1 yielding the desired articulation angle θ_{des}. Controller C_2 is a proportional controller which acts on the difference between the vehicle articulation angle θ and the desired articulation angle θ_{des} to yield the control action δ which serves as the input to the tractor.

The implementation of the controller design introduced in this section in PreScan tool is dealt with in the next section. For more details on the controller design and path description, the reader is advised to refer to the bibliography [3].

2.2.2 Blind Spot Detection

The Blind Spot Detection system, referred to as BSD, is a collision detection and avoidance system with passive (driver warning) and active (breaking autonomously) control actions. Blind spot is the area around a vehicle which is not visible from driver cabin. Any vehicle or pedestrian in this area will not be visible to the driver which may lead to wrong decisions causing accidents. According to a research conducted in Germany ([8]) in 2002 commercial vehicles were involved in 2920 accidents

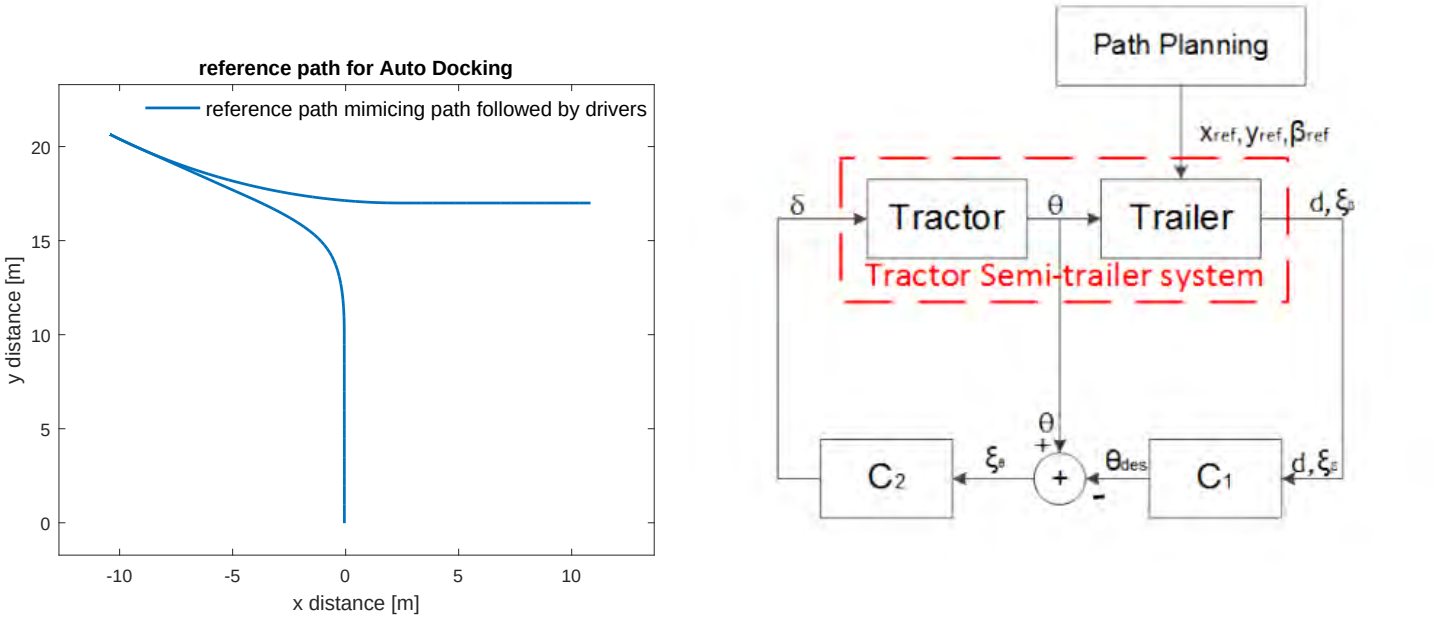

(a) Reference path used for Auto Docking simulation

(b) Cascade control scheme - Auto Docking [3]

Figure 2.3: Reference path and control scheme for Auto Docking

with cyclists and 1580 accidents with pedestrians which considered at a global level would be very high. Most of these accidents happen due to the aforementioned blind spot. Hence a lot of research is going on to detect this blind spot region with the help of sensors and develop of control algorithms to assist the driver and reduce the number of accidents. Figure 2.4 shows the blind spot area for BSD function development for urban setting (e.g. at traffic lights) as considered at DAF. The indirect field of vision correspond to the areas visible through mirrors on the vehicle.

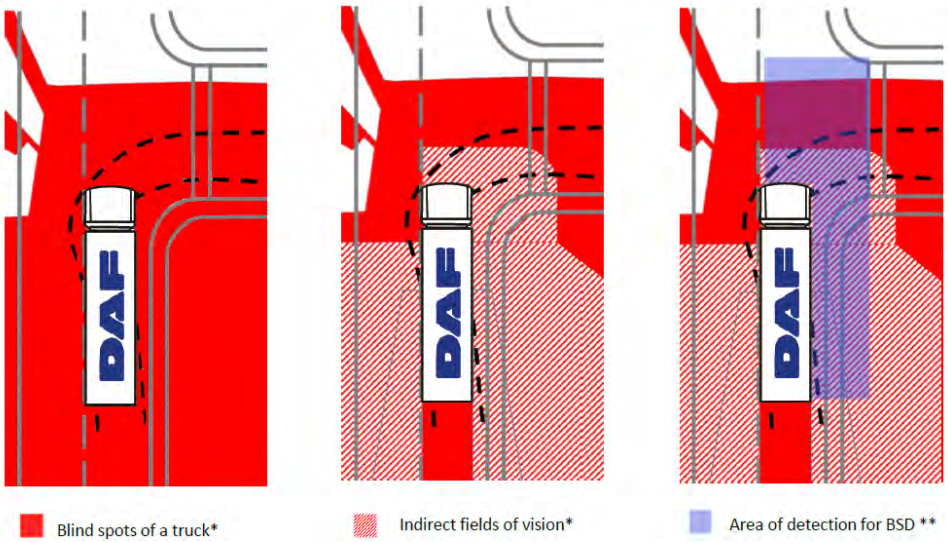

Figure 2.4: Blind Spot area for BSD function at DAF Courtesy: I. Surovtcev [12]

In figure 2.4, the blue area is the area of interest (AoI) for the BSD function development. To detect the AoI, the vehicle is fitted with two sensors - one stereo camera in front and one LIDAR on the co-driver side of the vehicle. The LIDAR has a range of 25 m with a horizontal field of view of 180 deg and vertical field of view of 5 deg. The angular resolution is 1 deg with an update rate of

60 ms. The stereo camera is 0.8 megapixels and has a resolution of $1024X768$ at 20 Hz frame rate. It has a horizontal field of view of 43 deg. The combined sensor field of view is shown in figure 2.5. The choice of sensors is based upon specific function requirements and budgetary constraints. The control logic behind BSD function can be categorized into three parts

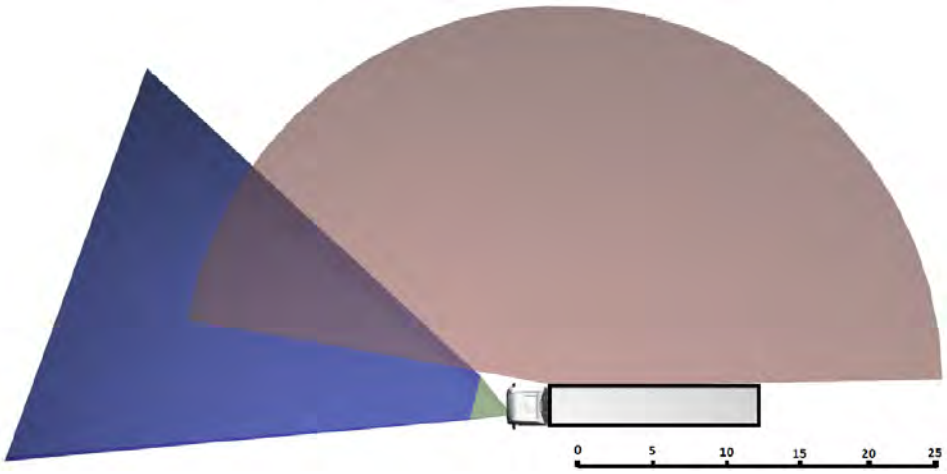

Figure 2.5: Overall sensor field of view [12]

1. If non-static objects i.e other vehicles or pedestrians are detected in the AoI, then the system **informs** the driver through a visual notification like a lit up panel in the driver cabin.
2. If non-static objects i.e other vehicles or pedestrians are detected in the AoI with the right turn signal on, the system **warns** the driver through visual and acoustic notifications.
3. If non-static objects (other vehicles or pedestrians) are detected in the AoI and the system predicts imminent collision beyond the driver's response time, the system **decelerates** the vehicle to a stop by sending a break signal to Electronic Brake System (EBS).

The case of imminent collision is based on **time to collision** computation based upon predicted trajectory of the non-static object. For prediction of the trajectory, information about the dimensions of the detected object together with object position, velocity and orientation is required from the sensors. If the time to collision goes below a certain threshold, the system activates braking. This project was performed for DAF by I. Surovtcev, another ASD student at Eindhoven University of Technology. For further details the reader is advised to refer to [12] in bibliography.

Implementation of BSD function in PreScan is discussed in the next section.

2.3 PreScan

PreScan is a simulation tool, provided by TASS International, aimed at developing ADAS systems with a range of sensors that can be used. It provides an interactive interface for creating real life scenarios to simulate test cases. It also provides a means to interact with pedestrians, other vehicles as well as infrastructure through communication modes namely, vehicle to vehicle (V2V) or vehicle to infrastructure (V2I), as well as build complex road networks.

One of the essential features of PreScan is the availability of sensor models that can be fitted to vehicles and buildings in the PreScan environment and simulated to obtain data that can be used for controller validation. The PreScan library contains some automotive sensors currently in the market like LIDAR (Light Detection and Ranging), camera, communication protocols, radar, etc. However

processing of the raw data for some of these sensors like LIDAR and radar, for example, is not available in PreScan and requires development of processing algorithms.

Due to the absence of sensor data processing algorithms, idealized sensors replace the LIDAR sensors in PreScan for the two ADAS functions being developed. These idealized sensors give the exact information about the detected objects in their field of view without the dynamics introduced by sensor technology used.

2.3.1 Simulation Objectives

Simulations are performed to evaluate PreScan as a tool for ADAS function development for DAF Trucks N.V. The objectives are subdivided into four main tasks as given below

1. Advantages of PreScan for ADAS function development.
2. Limitations of PreScan and possible solutions/workarounds.
3. Interfacing of Simulink models (kinematic and dynamic) with PreScan.
4. Implementation of Auto Docking and Blind Spot Detection in PreScan.

The subsequent sections deal with the objectives in order to provide practical insight to demonstrate the effectiveness of the tool for ADAS function development.

2.3.2 Advantages and Limitations: PreScan

Specific to the task of ADAS development of Auto Docking and Blind Spot Detection functions, PreScan has been evaluated using simulation models and has demonstrated certain advantages as well as limitations specific to the requirements of Vehicle Control Department at DAF.

The advantages of PreScan as seen through the implementation of Auto Docking and BSD function are listed below

- Import of complex road networks using `openstreetmaps.org`.
- Import of infrastructure from CAD files and Google Sketchup files.
- Actors like vehicles and pedestrians have their own set of dynamics which can be user defined
- Rich environment building as shown in figure 2.6.
- Vehicle state and steer information can be extracted for user defined paths.
- Availability of sensor models such as LIDAR, radar, camera, fish-eye camera, DSRC (Dedicated Short Range Communication) protocols, etc.
- Option of video capture from custom locations within the PreScan environment.

Despite the advantages there are a few limitations to the software in context of these functions which can be improved upon:

- Absence of separate trailer dynamics for tractor-trailer combinations. A workaround to this issue is discussed in the implementation of the Auto Docking process.
- Inferior visualization and animation properties of user imported actors. Active dialogue with parent company TASS is required for transfer of knowledge regarding correct import of user specific vehicles. Figures 2.7 compares the visual aspects of a default vehicle (top) in PreScan and a user imported vehicle (bottom). The result is achieved after multiple tries to retain the visual features of the vehicle in CAD.

Figure 2.6: Example of a built-in environment in PreScan

- No sensor processing algorithm in case of LIDAR and radar.
- Weather conditions do not affect LIDAR/radar readings automatically but need to be modelled in the sensors.

Figure 2.7: Visual difference between default and imported actors in PreScan

2.3.3 Interface between Simulink Model and PreScan

PreScan provides the capability of working with third party software packages, most importantly **Simulink** and **dSpace** which can be used to specify vehicle models and controller models for **actors** in PreScan. For simulation of given ADAS functions, Simulink is used. The interface from Simulink to PreScan is limited to the determination of spatial and velocity configuration of the actors excluding the rotational velocities. More specifically the information exchange is limited to the 9 parameters, as

shown in figure 2.8 which are position and velocity (along the three translation axes) and orientation (along the three rotational axes). The three rotational velocities are missing.

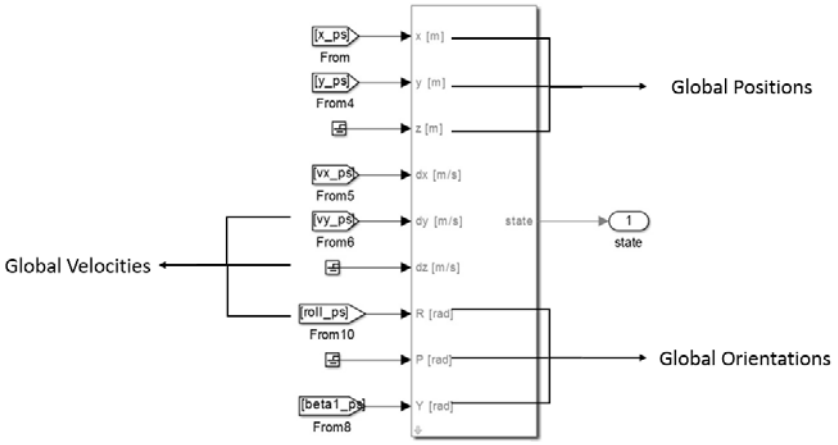

Figure 2.8: PreScan states for actors required form Simulink

2.3.4 Simulation of ADAS functions

Auto Docking

As discussed, PreScan allows for vehicles and pedestrians to be designed as **actors** with their own set of dynamics, driver model, trajectories to be followed and animation capabilities. One of the issues with using PreScan for implementation of Auto Docking function was the unavailability of separate trailer dynamics for the tractor-trailer combination. The default options available in PreScan restricted any modification to be made to the trailer dynamics which prevented the implementation of user specified models with their own dynamics.

To rectify the issue, rather than using the default tractor-trailer combination available in PreScan, the trailer is defined as a separate **actor** with its own dynamics fed to the tool using Simulink model. The model is based upon the nonlinear kinematic model as given in section 2.2. The model is built with appropriate interface to ensure plug and play approach for later simulations.

The Auto Docking simulation is shown in video 2.9. It is fast-forwarded for convenience. The video demonstrates the top view of the simulation for Auto Docking in a docking environment. The vehicle starts at some intial position in the neighborhood of the reference path and maneuvers to the final position by tracking the reference path. For details regarding controller performance reference is made to [6].

Blind Spot Detection

For implementation of BSD function in PreScan, the LIDAR is replaced by an idealized sensor that gives the required positional and kinematic configuration of the object within its field of view accurately. The test cases to be simulated are set in urban scenario and are shown in figure 2.10. The test case 1, as seen in PreScan environment, is shown in figure 2.11. The trajectories are synchronized at certain point in time which ensures a particular situation occurs without having to calculate the speed profiles for different **actors**. The simulation for this test case is shown in video 2.12 which only demonstrates the scenario. The simulation with controller design implemented is not shown because the controller design was in progress at the time of the project.

Figure 2.9: Simulation of Auto Docking in PreScan

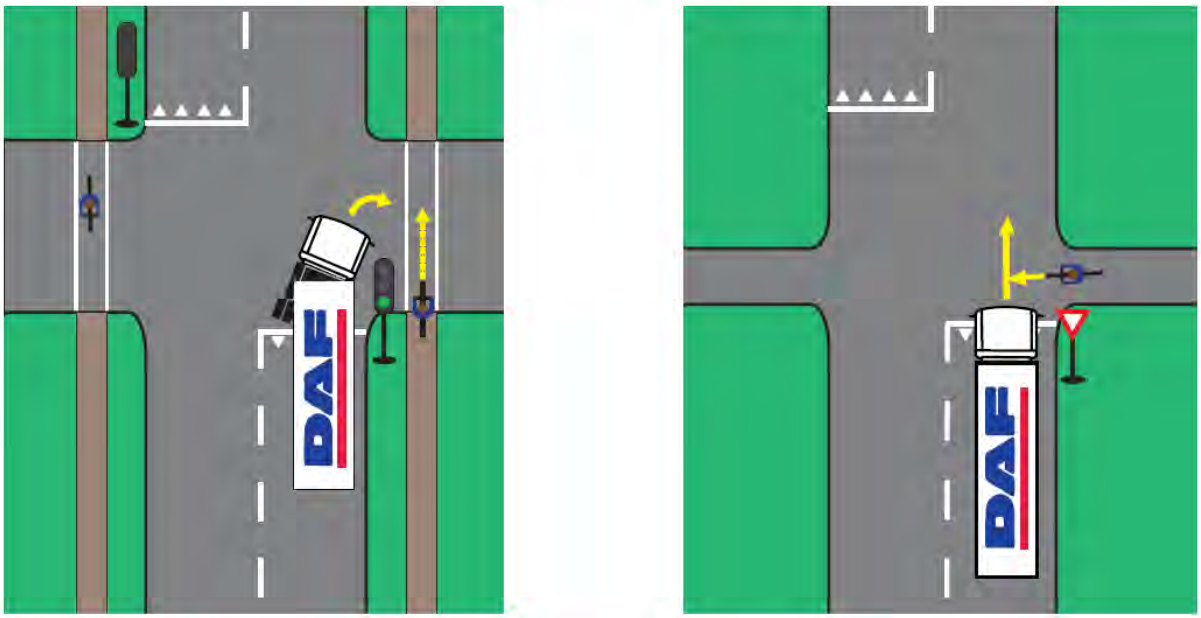

Figure 2.10: BSD test cases - Test Case 1 (1eft): cyclist coming from the right side of the truck and the truck makes a right turn; Test Case 2 (right): cyclist coming from right with the truck moving straight ahead

2.4 Conclusion

PreScan tool provides visualization for ADAS functions for user specified test cases which helps to understand behavior of the vehicle for a controller design. However the visual and animation effects are restricted for user imported vehicle models. One of three significant value additions, as per the two ADAS functions simulated, is the ability to build complex scenarios with rich environment as per the requirements of the test cases being simulated. The ability to import road networks and CAD models simplifies the task of scenario building to a large extent. The second significant value addition is the inclusion of sensor models which is extremely essential for ADAS functions. While some sensors can be directly used for function development, like a camera, others require the development of sensor data processing algorithms to be used for controller development like LIDAR and radar. In such a case, these actual sensors are replaced by idealized sensors that provide the

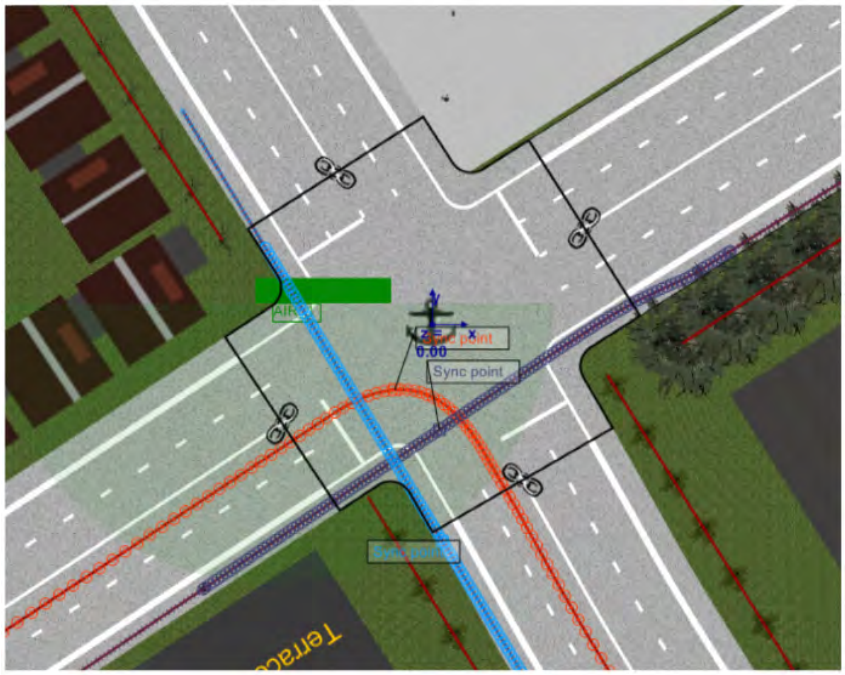

Figure 2.11: BSD test case 1 in PreScan - red trajectory for truck and purple trajectory for cyclist

required information. Thirdly, an advantage of PreScan is its integration with third party softwares like Simulink and dSpace since a lot of model development takes place in these environments. In a nutshell, PreScan allows for creation of scenarios with rich environment and hardware-in-loop simulations including sensors which is essential for virtual simulation of test cases and speeds up the function development process. The only significant drawbacks, from the controller development standpoint as seen with the simulation of two ADAS functions, is the requirement of sensor data processing algorithm for certain sensors and the absence of trailer dynamics for combined vehicle configurations.

Figure 2.12: Simulation of a test case for Blind Sport Detection

3. Lateral String Stability in Homogeneous Vehicle Platoons

The second part of the report deals with the investigation of conditions for lateral string stability in homogeneous vehicle platoons which is relatively unexplored in the research literature. This is part of a long term project **EcoTwin** at DAF aiming at vehicle platooning.

3.1 Introduction: Vehicle Platooning

Vehicle platooning is the future of transportation given the significant amount of benefits that can be drawn from it for all stakeholders involved. The trucks drive cooperatively at less than a second apart from one another using sensor technology and wireless communication with automated steering control and without human intervention (figure 3.13). This arrangement leads to lower fuel consumption and hence lower emissions due to decreased amount of aerodynamic drag. If safe platooning systems are developed only a single driver would be capable of leading a platoon where the following vehicles are autonomously driven. This would increase productivity since only one driver would be required to manage a platoon instead of several. Due to the omission of human induced errors it is expected to have fewer accidents and a more efficient utilization of existing road networks leading to less traffic jams and a better traveling experience.

Figure 3.13: Heterogeneous vehicle platooning

However, to realize this, a number of steps need to be taken by the society, government, industry and academia to ensure such benefits will become available. From a research standpoint, it is essential to demonstrate stability, safety and economic viability of such autonomous systems and as such a number of automotive companies across Europe are carrying out demonstrations to these effects.

Limitations to Lane Keeping Systems for Vehicle Platooning Application

The research on string stable unidirectional vehicle platooning in the longitudinal direction is extensive in literature. With advanced lane keeping algorithms in place, a string stable vehicle platoon should be capable of satisfactory vehicle following behavior in majority of highway conditions if not all. However there are two main drawbacks to this arrangement which are enumerated here

1. Uncertainty in case of faded lane markings or its absence altogether.

2. Lane change maneuver which conflicts with the primary objective of lane keeping systems.

The dependence of lane keeping system on road environment (lane markings) reduces the scope of operation of such platoons and falls short of providing a more generic stability criterion for lateral tracking based upon the interaction between vehicles in a platoon.

Very closely associated to the topic of vehicle platooning is the notion of string stability which is elaborated upon in the next section.

3.2 Notion of String Stability in Platooning

As stated before, the notion of string stability is extensive in research literature. As such a number of definitions exist. Unlike the conventional notion concerning evolution of states, string stability deals with the suppression of disturbances along a string of vehicles in a platoon. During earlier stages of research, string stability was conceived as a stability property in Swaroop and Hedrick (1996) in which a mathematical approach was adopted to derive sufficient conditions for asymptotic string stability implying uniform boundedness of all the states of an interconnected system for all time, given bounded initial conditions for a countably infinite vehicle string. One of the early works on the subject matter is given by Peppard (1974) in which conditions for string stability are investigated without inter-vehicular communication and it is shown that string stability can be achieved using spacing measurements for both preceding vehicle and following vehicle. In Yadlapalli et al (2006), string stability is analogous to the motion of a rigid body where under bounded disturbance forces the maximum deviation in motion of the string of vehicles is bounded and independent of the length of the string. In recent literature, string stability is mostly concerned with disturbance attenuation in states along the length of the string. In Ploeg et. al. (2014), the notion of $\mathscr{L}_2$ string stability is presented and conditions are derived for the $\mathscr{L}_2$ norm of error functions given the possibility of inter-vehicular communication and a $\mathscr{H}_\infty$ controller is designed to achieve $\mathscr{L}_2$ string stability.

The conventional Adaptive Cruise Control (ACC) system is supplemented with information from their surrounding vehicles (V2V) and infrastructure (V2I) to form what is known as Cooperative Adaptive Cruise Control (CACC). With the possibility of information exchange between vehicles, the notion of string stability as disturbance attenuation is explored in Naus et. al. (2010) for CACC systems. It is shown that string stable behavior can be achieved with a small inter-vehicular distance. Thus, a lot of research has already gone in investigation of string stability but there are still a lot of challenges towards achieving a such a vehicle capable of safely and efficiently interacting with its environment and taking decisions based on ethical nuances as human beings do.

In all the cases described in this section, the notion of string stability is explored for longitudinal control where the error to be minimized is the difference between existing inter-vehicular distance and desired inter-vehicular distance. However the notion of string stability for lateral tracking has not received much attention in literature. In the context of this report, string stability criterion is investigated for platoons in lateral direction by building upon the theory available for the longitudinal case.

3.3 Lateral String Stability

Longitudinal string stability, as discussed in literature, deals with disturbance attenuation along the vehicle string in longitudinal direction. To put it simply, the control scheme relies on wireless communication and sensor information to minimize a defined error to achieve string stability. Figure 3.14 shows a heterogeneous vehicle platoon with the three main ingredients for establishing string stability for the longitudinal control: feedforward control using wireless communication, feedback control signal (in this case the radar state) and an error to be minimized.

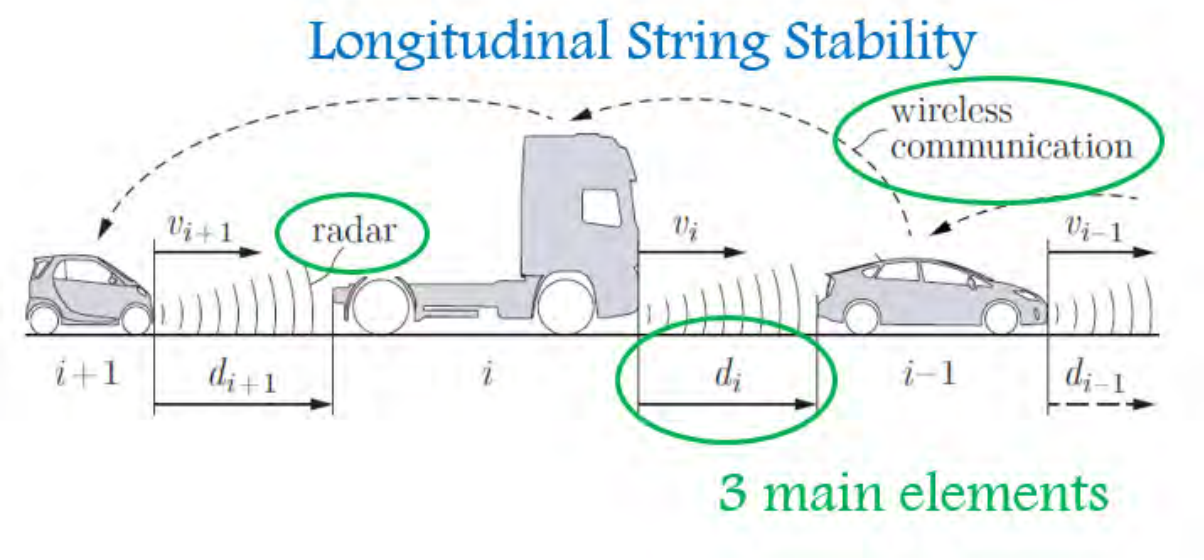

Figure 3.14: Heterogeneous vehicle platoon - important ingredients

A typical curve for string stability based upon the state of the system is shown in figure 3.15. The curve magnitude, which is the ratio of magnitude of states of following vehicle to the corresponding value for preceding vehicle, is less than or equal to 0dB for all input frequencies. It can be inferred from the figure 3.15 that this condition allows for tracking of low frequency behavior of the preceding vehicle while attenuating high frequent disturbances along the length of the string.

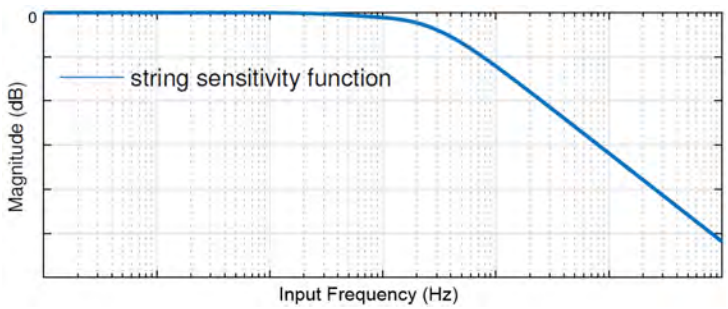

Figure 3.15: Typical output string stability sensitivity curve

Based upon the notion of string stability for longitudinal control, similar conditions can be derived for lateral control which, analogous to longitudinal string stability in platoon, allows for low frequent lateral motion tracking while attenuating high frequency disturbances based upon inter-vehicular communication over a wireless network in a cooperative environment. It is worthwhile to note a few differences between the longitudinal and lateral case from string stability standpoint.

1. For longitudinal string stability, the obvious choice for error minimization is based upon the inter-vehicular distance, d_i, for the i_{th} vehicle in a platoon. However the choice for lateral

string stability is not straightforward as will be made clear in the later sections of the report.

2. The previous argument also holds for the feedback signal to be used to achieve string stable behavior. This argument is an extension of the previous point.

3. In case of longitudinal string stability, the feedforward signal, vehicle acceleration, is communicated without delay in an ideal scenario. However for tracking purpose in lateral control, a delay is necessary to ensure that the feedforward input is applied not at the same time but at the same point in the trajectory in the ideal case.

4. For longitudinal string stability, the heading policy H_i (inter-vehicular spacing policy) provides an important tuning parameter to achieve string stability. It is shown in Naus et. al. [5] that with constant inter-vehicular distance $H = 1$ string stability cannot be guaranteed. This becomes more clear when the string stability transfer function is analyzed

$$SS_i = \frac{G_i K_i}{1 + H_i G_i K_i} = T_i \tag{3.1}$$

where G_i denotes the plant transfer function, K_i denotes the controller transfer function and H_i denotes the heading policy. SS_i and T_i are the string sensitivity and complementary sensitivity functions respectively. In absence of H_i, string stability cannot be guaranteed due to the water-bed effect for systems with relative degree 2. Hence H_i provides a handle to the sensitivity function. For lateral case, such a parameter may not exist. The possibility of replacing the heading policy for the lateral case is open to exploration.

Taking these points into consideration, in subsequent sections, conditions are derived for lateral string stability for a **homogeneous vehicle platoon** and investigated taking the theory for longitudinal string stability as a reference. Furthermore, the similarities and in specific dissimilarities between the two are analysed with the objective of providing insight into the design of controllers to achieve lateral string stability.

3.4 Vehicle Model

The vehicle model used for simulation in the report is taken from the ASD project on Active Lane Change Assist System (ALKAS) by A.D. George [4]. Certain assumptions have been made to simplify the analysis, given the focus of the project, so that conclusions can be drawn based upon a simplistic model, which can be extended to a complex nonlinear model at a later stage.

3.4.1 Assumptions

Following assumptions are made when deriving the bicycle model of the tractor-trailer combination.

1. The lateral dynamics of a vehicle is dependent on the longitudinal velocity but treating it as a varying parameter makes the lateral dynamics nonlinear and complicates the stability analysis. For simplicity, the lateral vehicle model considered in this report assumes constant longitudinal velocity u.

2. The tire model is assumed to be linear which constant cornering stiffness coefficient. During highway application this assumption holds since the steering maneuvers lie within the linear region of the tire force curve.

3. Only level road surfaces are considered.

4. Weight transfer effects in both longitudinal and lateral directions are not considered.

5. For simplicity of the analysis only homogeneous platoons are considered.

6. It is assumed that the distance between the vehicles is constant which is acceptable given the assumption of a constant longitudinal velocity and comparatively small lateral velocities.

Consider the vehicle model as shown in figure 3.16. The derived equations of motion of the system are based on paper by M. El-Gendy ([3]). Table A.1 list the symbolic notations used for the derivation of the bicycle model along with the values used for the model.

For equilibrium in the lateral direction for the tractor center of gravity and assuming small angles

$$m_1\ddot{y}_1 + m_1 u\dot{\phi}_1 = F_{y1} + F_{y2} - F_{hitch}$$

For moment equilibrium about the tractor center of gravity

$$I_{zz1}\ddot{\phi}_1 = l_1 F_{y1} - l_2 F_{y2} + l_6 F_{hitch}$$

Similarly, the equilibrium equations for lateral direction and moment around the vertical axis, respectively, for trailer center of gravity are given by

$$\begin{aligned} m_2\ddot{y}_2 + m_2 u\dot{\phi}_2 &= F_{y3} + F_{y4} + F_{y5} + F_{hitch} \\ I_{zz2}\ddot{\phi}_2 &= -l_3 F_{y3} - l_4 F_{y4} - l_5 F_{y5} + l_7 F_{hitch} \end{aligned}$$

To eliminate the unknown parameter F_{hitch}, the coupling equations as derived in [3] can be used as given by

$$\dot{y}_2 + l_7\dot{\phi}_2 = \dot{y}_1 - l_6\dot{\phi}_1 + u\theta$$

Rewriting $\theta = \phi_1 - \phi_2$ and differentiating,

$$\ddot{y}_2 + l_7\ddot{\phi}_2 + u\dot{\phi}_2 = \dot{y}_1 - l_6\dot{\phi}_1 + u\dot{\phi}_1$$

Also, the lateral tire force at the i_{th} axle, F_i is assumed to be linearly dependent on the side slip angle, α_i

$$F_{yi} = C_i\alpha_i$$

where the proportional coefficient C_i is the cornering stiffness at the axle.
For small angles, the tire slip angles α_i can be approximated by

$$\begin{aligned} \alpha_1 &= \delta - \frac{\dot{y}_1 + l_1\dot{\phi}_1}{u} \\ \alpha_2 &= -\frac{\dot{y}_1 - l_2\dot{\phi}_1}{u} \\ \alpha_3 &= -\frac{\dot{y}_2 - l_3\dot{\phi}_2}{u} \\ \alpha_4 &= -\frac{\dot{y}_2 - l_4\dot{\phi}_2}{u} \\ \alpha_5 &= -\frac{\dot{y}_2 - l_5\dot{\phi}_2}{u} \end{aligned}$$

Using the equations above and after some mathematical manipulation of the equation of motion, the resultant vehicle model is given by

$$M\dot{x} = Ax + Bu \tag{3.2}$$

where $x = [\dot{y}_1, \dot{\phi}_1, \dot{y}_2, \dot{\phi}_2]^T$ and $u = \delta$.

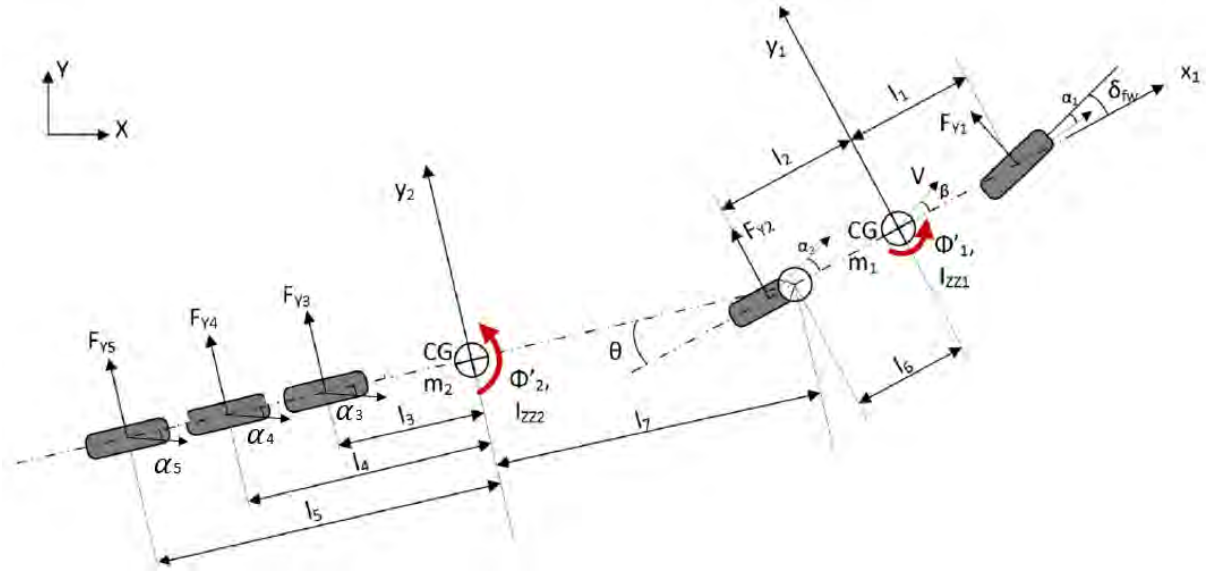

Figure 3.16: Bicycle model for tractor-trailer combination. [4]

The M, A and B matrices are given by

$$M = \begin{pmatrix} m_1 & 0 & m_2 & 0 \\ 0 & I_{zz1} & -l_6 m_2 & 0 \\ 0 & 0 & -l_7 m_2 & I_{zz2} \\ 1 & -l_6 & -1 & l_7 \end{pmatrix} \qquad B = \begin{pmatrix} C_1 \\ C_1 l_1 \\ 0 \\ 0 \end{pmatrix}$$

$$A = \begin{pmatrix} A_{11} & A_{12} & A_{13} & A_{14} \\ A_{21} & A_{22} & A_{23} & A_{24} \\ 0 & 0 & A_{33} & A_{34} \\ 0 & -u & 0 & u \end{pmatrix}$$

where

$$\begin{aligned} A_{11} &= \frac{(-C_1 - C_2)}{u} \\ A_{12} &= \frac{(-C_1 l_1 + C_2 l_2)}{u} - m_1 u \\ A_{13} &= \frac{-C_3 - C_4 - C_5}{u} \\ A_{14} &= \frac{C_3 l_3 + C_4 l_4 + C_5 l_5}{u} - m_2 u \\ A_{21} &= \frac{-C_1 l_1 + C_2 l_2}{u} \\ A_{22} &= \frac{-C_1 l_1^2 - C_2 l_2^2}{u} \\ A_{23} &= \frac{C_3 l_6 + C_4 l_6 + C_5 l_6}{u} \\ A_{24} &= \frac{-C_3 l_3 l_6 - C_4 l_4 l_6 - C_5 l_5 l_6}{u} + l_6 m_2 u \\ A_{33} &= \frac{C_3 l_7 + C_4 l_7 + C_5 l_7 + C_3 l_3 + C_4 l_4 + C_5 l_5}{u} \\ A_{34} &= \frac{-C_3 l_3^2 - C_4 l_4^2 - C_5 l_5^2 - C_3 l_3 l_7 - C_4 l_4 l_7 - C_5 l_5 l_7}{u} + l_7 m_2 u \end{aligned} \tag{3.3, 3.4}$$

The outputs of the model, for the upcoming analysis, are limited to the tractor lateral velocity, v_1 and yaw rate $\dot{\phi}_i$. For the validation of the model the reader is advised to refer to the bibliography [4]. The model is extended to include additional outputs in the next section and used for deriving conditions for lateral string stability.

3.5 Preliminary Work

As discussed in section 3.3, one of the major differences between longitudinal string stability and its lateral counterpart is the obvious choice of control error for minimization in the longitudinal case. Since such a choice is not as straightforward for the lateral case, the first task is to define the error to be minimized for the control objective. Figure 3.17 represents the signals involved in lateral string stability analysis. Since only homogeneous platoons are considered, the feedforward signal can be taken as the steering angle input δ. For feedback control, lateral velocity v, yaw rate $\dot{\phi}$ and sensor state y_L are considered. The error in these cases are error in lateral velocity, error in yaw rate and error in sensor state respectively. The reference signals from preceding vehicle to calculate errors in lateral velocity and yaw rate for the following vehicle can be measured using advanced sensor technologies, which not a part of this report, or can be communicated over wireless network. In either case, it is assumed that these reference signals from the preceding vehicle are available.

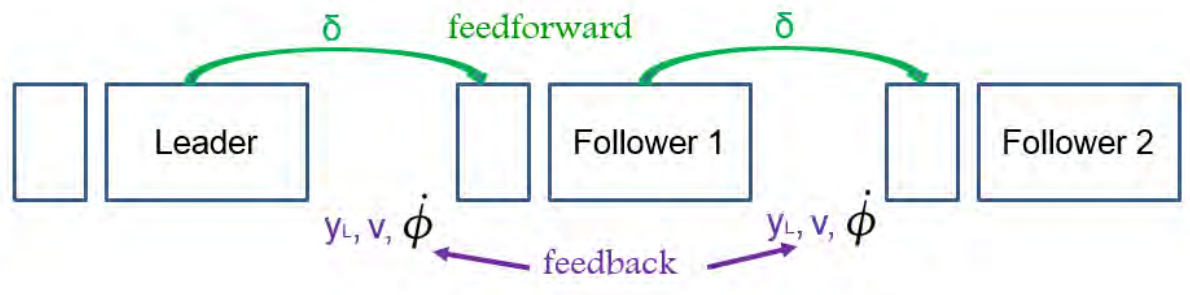

Figure 3.17: Ingredients for lateral string stability

Before starting with the derivation of lateral string stability condition, some preliminary work is required. A reference path is designed for the leader of the platoon to follow. Using PreScan tool it is possible to perfectly track a reference path built into its environment and, thus, it can be safely assumed that the leader does so. As stated in section 3.4.1 the leader is assumed to have a constant longitudinal velocity of 15m/s. In order to approximate highway conditions, a radius of 200 m is considered which limits the lateral acceleration of the vehicle to around 1.125 m/s^2. Given the dimensions of the vehicle concerned (refer to appendix A.1), a longitudinal distance of 15 m is considered. For sensor state, the lateral offset of the preceding vehicle is considered. It is defined as the offset between the center of gravity of the preceding vehicle and the vehicle center-line of the following vehicle. The forward looking sensors like radar, LIDAR, etc. can provide the rear-most position of the preceding vehicle accurately. With communication it is possible to include information about the heading angle of the preceding vehicle and calculate the lateral offset as defined in this case. Referring to figure 3.18(a), the assumption of a constant longitudinal velocity and hence constant inter-vehicular distance, d, makes the parameters - lateral offset (y_L) and angle between the vehicles (θ), linearly dependent on each other. The reference path followed by the leader is shown in figure 3.18b.

For the preliminary work a simple two vehicle platoon is considered.

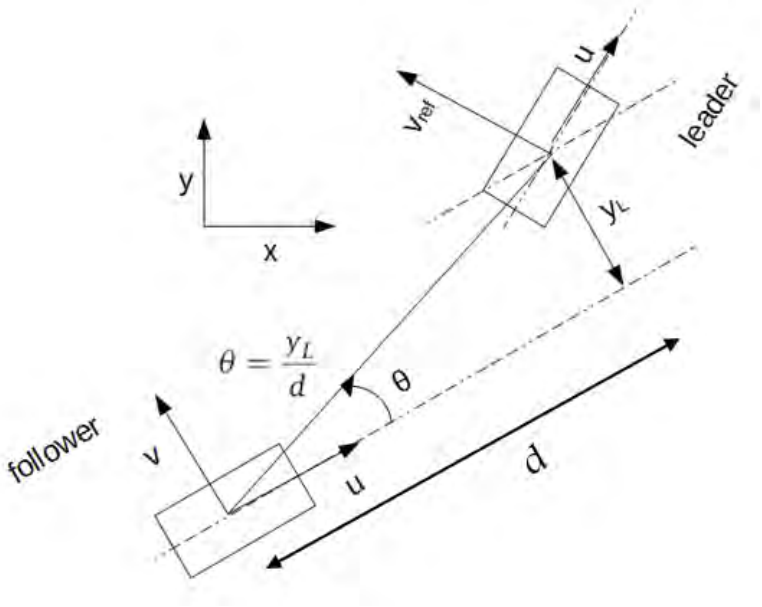

(a) Sensor state

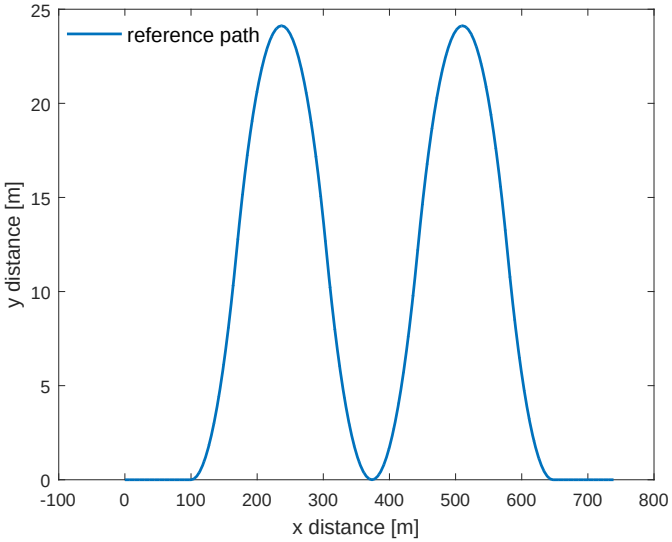

(b) Reference Path

Figure 3.18: Sensor state and reference path followed by the platoon leader

3.5.1 Feedforward Control

The steering input from the preceding vehicle is fed to the follower vehicle with a delay. The necessity of the delay arises due to the constant inter-vehicular distance between the vehicles (d) which is given by

$$\tau = \frac{d}{u}$$

where u is the constant longitudinal velocity. Intuitively, it becomes obvious to introduce this delay since the steer inputs for path tracking depends upon the vehicle position on the track and therefore needs to be delayed till the follower vehicle reaches the referred position.

Simulation and Results

The simulation is carried out and the results are plotted in 3.19. It should be noted that no limitations are imposed on steering angle and rate of change of steering angle for these simulations. As expected, without any disturbances the vehicles perfectly track the reference path with feedforward.

3.5.2 Estimation of Lateral Offset of the Preceding Vehicle

Given the assumption of constant inter-vehicular distance, the information from most forward looking sensors (LIDAR, vision based sensors, radars, etc.) would be limited to the lateral offset with respect to the following vehicle. To derive the dynamics associated with the estimation of the lateral offset of the preceding vehicle, consider two vehicles in a platoon as shown in figure 3.20. Let the following vehicle have a lateral velocity v with respect to body fixed coordinate system and heading angle ϕ. Similarly let the corresponding parameters for the preceding vehicles be v_{ref} and ϕ_{ref} respectively. The relative motion in lateral direction can then be described by the following equation

$$\dot{y}_L = v_{ref} \cdot cos(\phi_{ref} - \phi) + u \cdot sin(\phi_{ref} - \phi) - v - d\dot{\phi} \tag{3.5}$$

when d is the constant longitudinal inter-vehicular distance. Assuming small difference in the orientation between two consecutive vehicles in a platoon i.e. $\phi_{ref} - \phi << 1$, (3.5) reduces to the following linear form

$$\dot{y}_L = v_{ref} + u(\phi_{ref} - \phi) - v - d\dot{\phi} \tag{3.6}$$

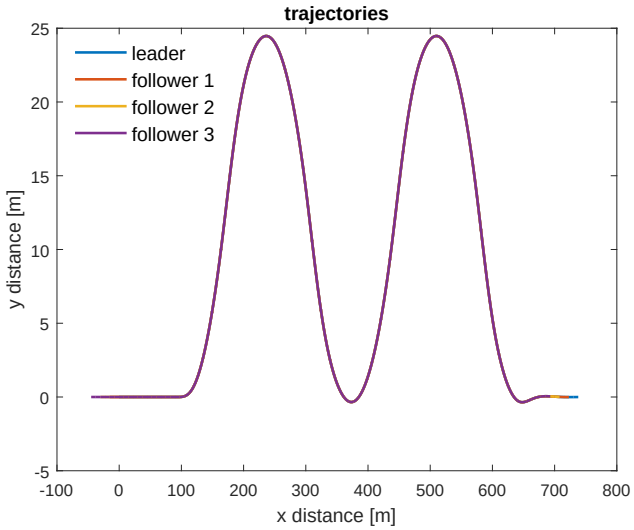

Figure 3.19: Vehicle tracking with perfect feedforward

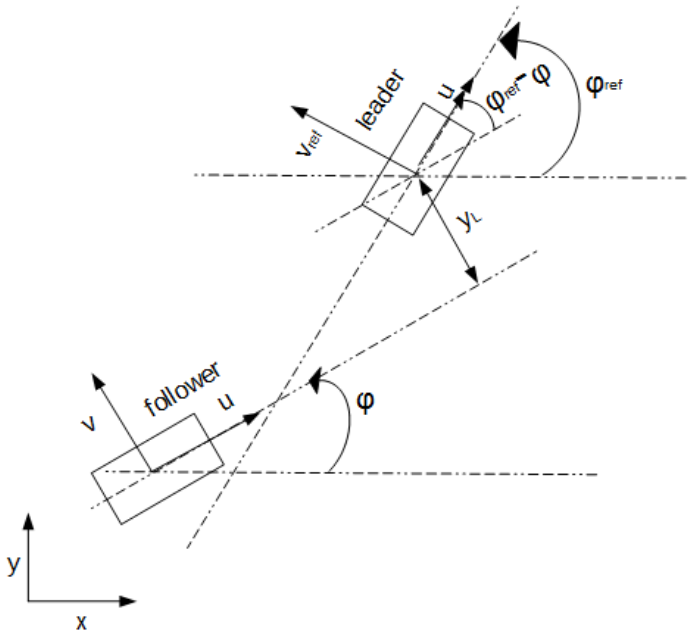

Figure 3.20: Derivation of lateral offset, y_L

where the integration of the parameter $\dot{y}_L$ gives the lateral offset of the preceding vehicle with respect to the following vehicle. Figure 3.21 compares the lateral offset estimation using (3.6) and actual offset calculated using position coordinates of the two vehicles and shows a promising result.

The vehicle model is extended with state y_L. Furthermore the lateral velocity (v_{ref}) and heading angle (ϕ_{ref}) of the preceding vehicle are included in the model as reference inputs. The appended model takes the form

$$M_a\dot{X} = A_aX + B_au_a \tag{3.7}$$

where $X = [y_1, \dot{y}_1, \phi, \dot{\phi}_1, \dot{y}_2, \dot{\phi}_2, y_L]^T$ and $u_a = [\delta, \phi_{ref}, v_{ref}]^T$.

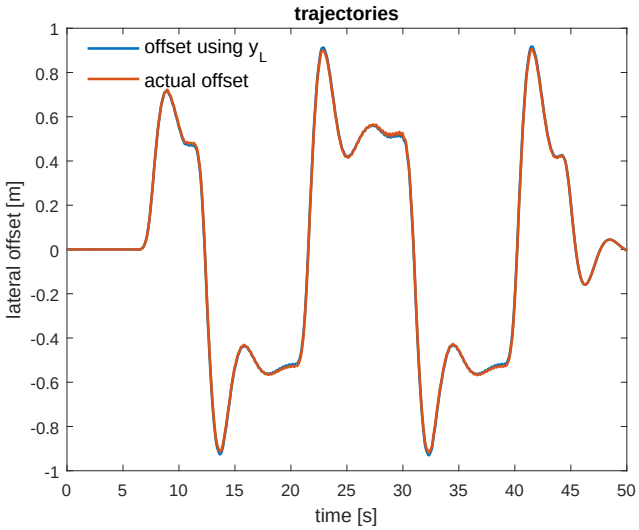

Figure 3.21: Comparison between y_L estimate and actual offset calculated using position of vehicles in simulation

$$M_a = \begin{pmatrix} 1 & 0 & 0 & 0 & 0 & 0 & 0 \\ 0 & m_1 0 & & 0 & m_2 & 0 & 0 \\ 0 & 0 & 1 & 0 & 0 & 0 & 0 \\ 0 & 0 & 0 & I_{zz1} & -_6 m_2 & 0 & 0 \\ 0 & 0 & 0 & 0 & -l_7 m_2 & I_{zz2} & 0 \\ 0 & 1 & 0 & -l_6 & -1 & l_7 & 0 \\ 0 & 0 & 0 & 0 & 0 & 0 & 1 \end{pmatrix} \qquad B_a = \begin{pmatrix} 0 & 0 & 0 \\ C_1 & 0 & 0 \\ 0 & 0 & 0 \\ C_1 l_1 & 0 & 0 \\ 0 & 0 & 0 \\ 0 & 0 & 0 \\ 0 & u & 1 \end{pmatrix}$$

$$A_a = \begin{pmatrix} 0 & 1 & 0 & 0 & 0 & 0 & 0 \\ 0 & A_{11} & 0 & A_{12} & A_{13} & A_{14} & 0 \\ 0 & 0 & 0 & 1 & 0 & 0 & 0 \\ 0 & A_{21} & 0 & A_{22} & A_{23} & A_{24} & 0 \\ 0 & 0 & 0 & 0 & A_{33} & A_{34} & 0 \\ 0 & 0 & 0 & -u & 0 & u & 0 \\ 0 & -1 & -u & -L_f & 0 & 0 & 0 \end{pmatrix}$$

where terms A_{11}, A_{12}, A_{13}, A_{14}, A_{21}, A_{22}, A_{23}, A_{24}, A_{33} and A_{34} are given in (3.3) to (3.4). The output space is also appended with lateral offset y_L.

3.5.3 Reference Generation for Lateral Offset y_L

Now that the lateral offset y_L has been estimated, it can be used to create a feedback controller for vehicle platooning. However using y_L as the control error poses two major issues. First, in absence of feedforward, a controller based upon lateral offset is prone to corner cutting behavior which is not desirable for the platoon stability. This behavior is demonstrated in figure 3.22(a). Secondly, while going along a curve, a lateral offset must exist between two vehicles in a platoon. However a controller based upon y_L would treat this necessary offset as an error and try to minimize it causing the vehicle to deviate from the path to be tracked. Figure 3.22(b) shows that the tracking performance, with feedforward, is hampered due to this effect.

To resolve these issues, it is possible to use the yaw information from the preceding vehicle to generate a reference profile for lateral offset y_L to track. Consider two vehicles in a platoon driving on a curved path with a fixed radius R as shown in figure 3.23. It should be noted that the representation is exaggerated and the curved length between the two vehicles and distance, d, are

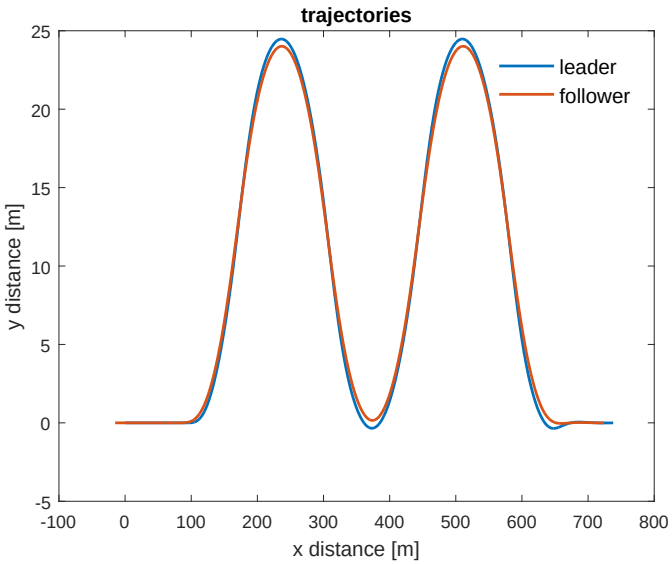

(a) Corner cutting behavior for controller based on y_L

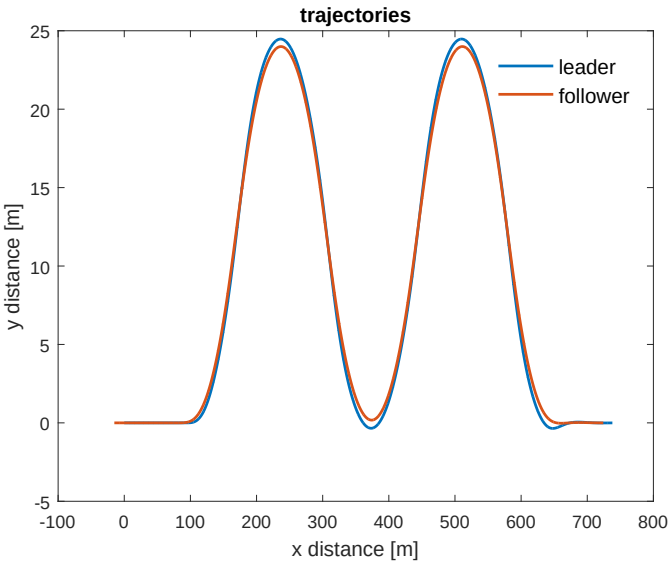

(b) Performance deterioration in presence of feedforward

Figure 3.22: Issues with feedback control based upon lateral offset y_L as the control error

equal for very small curvatures. At steady state, the yaw rate of the vehicle is related to the the longitudinal velocity and radius of turn and the relation is given by

$$\dot{\phi} = \frac{u}{R} \tag{3.8}$$

where u is the constant longitudinal velocity.

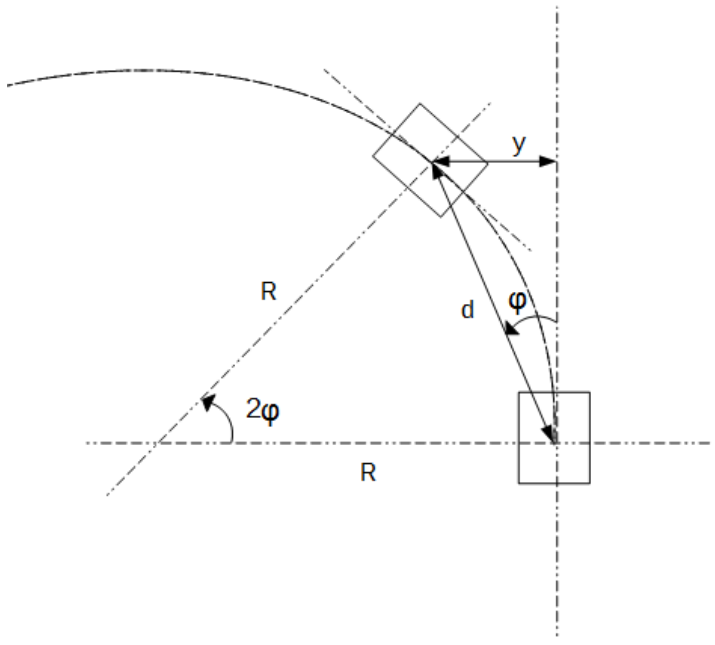

Figure 3.23: Lateral offset estimate based on yaw rate

Thus using relation (3.8), the yaw rate information can be used to estimate lateral offset y. From the figure 3.23, it is apparent that the following relation holds for small angle ϕ

$$2\phi = \frac{d}{R} \tag{3.9}$$

$$\implies 2\frac{y}{d} = \frac{d}{R} \tag{3.10}$$

$$\implies y = \frac{d^2}{2R} \tag{3.11}$$

$$\implies y = \frac{d^2}{2\left(\frac{u}{\dot{\phi}}\right)} \tag{3.12}$$

It should be noted that the lateral offset derived in (3.12) is for steady state conditions. To compensate for the error induced due to this, reference for lateral offset can be shaped such that it builds up to the steady state value given by (3.12) using a second order filter K_c. After some tuning of the filter K_c, it is given by

$$K_c = \frac{1}{0.5s^2 + s + 1} \tag{3.13}$$

The improvement in tracking performance is demonstrated in figure 3.24. Details regarding the need of filter K_c and its design can be found in appendix A.2.

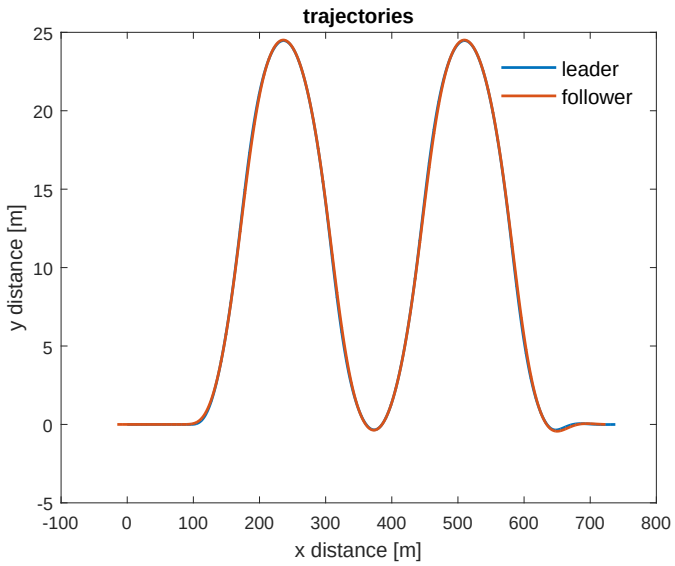

Figure 3.24: Performance after using yaw rate information from preceding vehicle to generate a reference for lateral offset y_L

This implies that the compensation instantly goes to steady state value while the actual vehicle builds up to this value.

In the next sections the conditions for achieving string stability for lateral dynamics are derived and subsequently string stable controllers are designed based upon these conditions.

3.5.4 Summary

In this section, a feedback controller based upon lateral offset measurement is designed. Since such a feedback controller uses the error at the look-ahead distance, so the vehicle cuts corners which would be unacceptable for vehicle following in a highway setup and this effect needs to be minimized. Moreover, in combination with feedforward, additional input provided by the feedback

controller yields, comparatively, poor tracking results. Consequently, a reference is generated based on yaw rate information of the preceding vehicle for the lateral offset y_L to track. This resulted in significant improvement in tracking performance.

3.6 Conditions for Lateral String Stability: Frequency Domain Approach

In order to understand the limitation on controller design for lateral tracking in a homogeneous platoon, analogous to longitudinal string stability, conditions for lateral string stability need to be derived to give a better understanding of the limitations posed on controller design for acceptable platoon behavior.

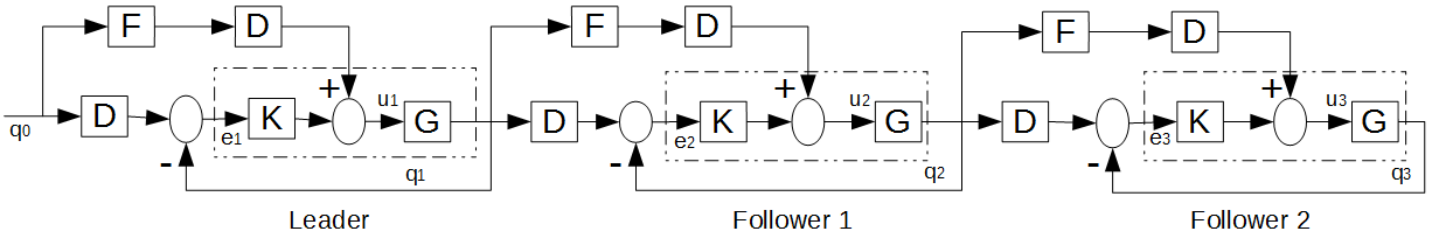

Figure 3.25: Control scheme of a platoon consisting of 3 vehicles. Notations - D: delay function, K: controller, F: feedforward filter, G: plant(vehicle)

In figure 3.25, following notations are used

- q_i - model outputs (lateral offset(y_L), lateral velocity(v) and yaw rate of the tractor $\dot{\phi}$)
- e_i - corresponding error signal
- u_1 - input signal i.e. steering angle

Consider the control scheme for a short platoon consisting of three vehicles as shown in figure 3.25. From the diagram, ignoring feedforward for the leading vehicle, consider the following set of relations

$$e_1 = Dq_0 - q_1 \tag{3.14}$$
$$e_1 = Dq_0 - Gu_1 \tag{3.15}$$
$$e_1 = Dq_0 - G(DFq_0 + Ke_1) \tag{3.16}$$
$$(1+GK)e_1 = (D - GDF)q_0 \tag{3.17}$$
$$\frac{e_1}{q_0} = S(D - GDF) \tag{3.18}$$

where $S = \dfrac{1}{1+GK}$ is the local sensitivity function for the considered closed loop.

Similarly, for the second vehicle we obtain

$$\frac{e_2}{q_1} = S(D - GDF) \tag{3.19}$$

The relation between subsequent error profiles is given by

$$\frac{e_2}{q_1} = \frac{e_1}{q_0} \tag{3.20}$$
$$\frac{e_2}{e_1} = \frac{q_1}{q_0} \tag{3.21}$$
$$\tag{3.22}$$

This series of relations can be similarly derived for a platoon of infinite length. Consider such a platoon, for the i_{th} vehicle in a platoon, the following relationships hold

$$\frac{e_i}{q_{i-1}} = S(D - GDF) \tag{3.23}$$

$$\frac{e_i}{e_{i-1}} = \frac{q_{i-1}}{q_{i-2}} \tag{3.24}$$

For lateral string stability of a platoon of infinite length, the error profile must not amplify from leading vehicle to vehicles following in the platoon. Analogous to the string stability condition for longitudinal control, the condition for string stability can be written as

$$|\hat{SS}_i| = \left|\frac{e_i}{e_1}\right| \leq 1, \forall \omega \tag{3.25}$$

where $\hat{SS}_i$ is the so-called string stability transfer function.
In the considered scenario only communication with the preceding vehicle is considered and thus the condition for lateral string stability can be written as

$$|SS_i| = \left|\frac{e_i}{e_{i-1}}\right| = \frac{q_{i-1}}{q_{i-2}} \leq 1, \forall \omega \tag{3.26}$$

It should be noted that the condition given by equation 3.26 is more conservative and its satisfaction automatically implies the satisfaction of condition given by equation 3.25 which from hereon would be referred to as the **conservative lateral string stability** condition.

However, the conservative string stability condition described above compares the error profiles between consecutive vehicles but does not describe the absolute error in position with respect to the initial reference trajectory. It is possible that the error relative to the preceding vehicle goes on decreasing along the string length but keeps increasing at an ever decreasing rate with respect to reference trajectory. This particular case is shown in figure 3.26 where despite error with respect to preceding vehicle decreasing, it is increasing in relation to global reference. Therefore, it is imperative to look at the error in trajectory of a vehicle in a platoon in relation to the reference trajectory.

The relation between **global** error for the i_{th} vehicle in a platoon and the initial reference q_0 is defined as

$$\frac{e_{i,0}}{q_0} = \frac{q_0 - q_i}{q_0} \tag{3.27}$$

Thus,

$$\hat{SS}_{i,g} = \frac{e_{i,0}}{q_0} = 1 - \frac{q_i}{q_0} \tag{3.28}$$

Again referring to figure 3.25, consider the following set of relations for the leader of the platoon with no feedforward signal,

$$\begin{aligned} q_1 &= Gu_1 \\ q_1 &= G(DFq_0 + Ke_1) \end{aligned}$$

For the first vehicle in the platoon $F = 0$ since there is no feedforward,

$$\begin{aligned} q_1 &= G(DFq_0 + Ke_1) \\ q_1 &= GK(Dq_0 - q_1) \\ q_1 &= GKDq_0 - GKq_1 \\ (1 + GK)q_1 &= GKDq_0 \\ \frac{q_1}{q_0} &= SGKD \end{aligned}$$

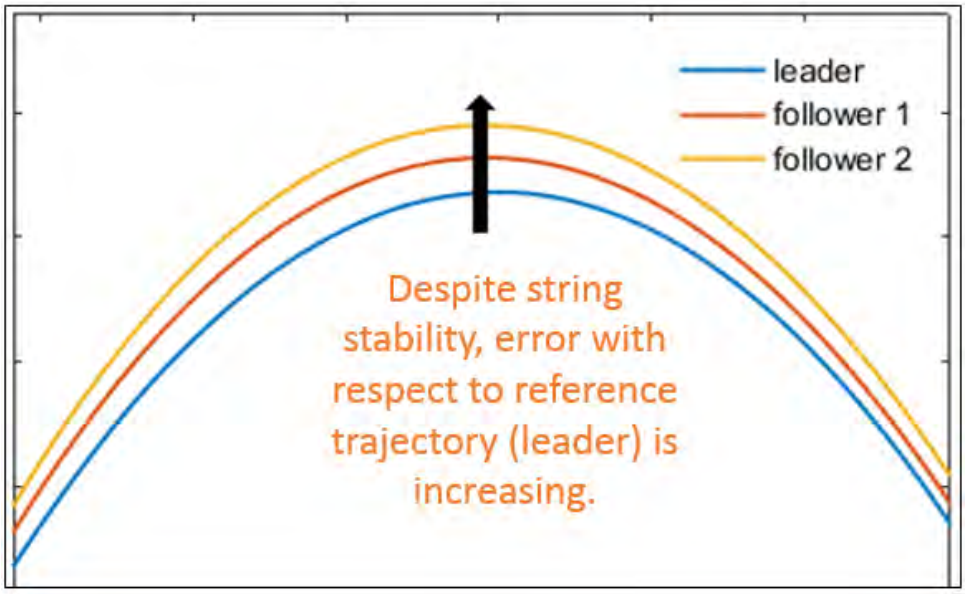

Figure 3.26: Increase in error w.r.t. reference despite string stability

For the subsequent vehicle in the platoon, the same set of relations (note that now there is also a feedforward signal) are given by

$$\begin{aligned} q_2 &= Gu_2 \\ q_2 &= G(Ke_2 + DFq_1) \\ q_2 &= G(K(Dq_1 - q_2) + DFq_1) \\ q_2 &= G(KDq_1 - Kq_2 + DFq_1) \\ (1+GK)q_2 &= (GKD + GDF)q_1 \\ \frac{q_2}{q_1} &= SG(KD + DF) \end{aligned}$$

where F is the feedforward filter.

For a platoon of infinite length, the above relationship can be written as

$$\frac{q_i}{q_{i-1}} = SG(KD + DF) \qquad \text{for } i > 1 \tag{3.29}$$

Moreover, on account of homogeneity of the system, the relation between the states of i_{th} vehicle to the reference states is given by

$$\frac{q_i}{q_0} = (SG(KD + DF))^{i-1} \cdot \frac{q_1}{q_0} \tag{3.30}$$

$$\frac{q_i}{q_0} = (SG(KD + DF))^{i-1} \cdot SGKD \tag{3.31}$$

Using the result obtained in (3.29), the condition for conservative string stability given by (3.26) can be rewritten as

$$|SS_i| = \left|\frac{e_i}{e_{i-1}}\right| = |SG(KD + DF)| \leq 1, \qquad \forall \omega \ \& \ i > 1 \tag{3.32}$$

The relation between **global** error and reference trajectory as given by (3.28) can be rewritten based upon the state equation given by (3.31),

$$\hat{SS}_{i,g} = \frac{e_{i,0}}{q_0} = 1 - (SG(KD + DF))^{i-1} \cdot SGKD \quad \forall \omega \tag{3.33}$$

Lateral String Stability: With Combined Feedforward and Feedback

In case of a perfect feedforward, $F = G^{-1}$ i.e. the feedforward filter is equal to the inverse of the plant. Putting the expression for feedforward filter in (3.32) reduces it to the following expression

$$|SS_i| = |SG(KD + DG^{-1})|, \qquad \forall\omega \;\&\; i > 1 \tag{3.34}$$
$$|SS_i| = |S(GK + 1)D|, \qquad \forall\omega \;\&\; i > 1 \tag{3.35}$$
$$|SS_i| = |D| = 1, \qquad \forall\omega \;\&\; i > 1 \tag{3.36}$$

Therefore, only marginal stability can be achieved leaving the system vulnerable to uncertainties or modeling errors. Given the relation above, error profiles vanish as substitutions in (3.33) demonstrate.

$$|\hat{SS}_{i,g}| = |1 - (SG(KD + DG^{-1}))^{i-1} \cdot SGKD| = |1 - SGKD|, \qquad \forall\omega \tag{3.37}$$

where the latter equation implies that, for all vehicles in platoon behind the leading vehicle, the error is identically equal to the error with which the leading vehicle tracks the reference trajectory.

Lateral String Stability: With Feedback only

In absence of feedforward, the conservative lateral string stability condition (3.26) reduces to the following form

$$SS_i = SGKD, \qquad \forall\omega \;\&\; i > 1 \tag{3.38}$$

And the ratio of global error and reference state is given by

$$\hat{SS}_{i,g} = 1 - (SGKD)^i, \qquad \forall\omega \tag{3.39}$$

The equation would be referred to as **global sensitivity function** from hereon.

In the next section, using the conditions given by equations (3.38) and (3.39), feedback controllers are designed to achieve lateral string stability.

3.7 Controller Design and Lateral String Stability

The condition derived for lateral string stability in section 3.6 provides guidelines for the design of controller to achieve a lateral string stable vehicle platoon. This section explores the possibility of a feedback controller based on error in vehicle states and lateral offset y_L satisfying the derived lateral string stability condition. The effect on the so-called global string sensitivity function $\hat{SS}_{i,g}$ will also be analyzed.

3.7.1 Lateral Offset Based Feedback Controller

For design based on lateral offset y_L, the feedback controller minimizes the difference between the reference state as discussed in section 3.5 and lateral offset y_L and produces the requisite control action. Using the parameters given in Table A.2 in appendix A.1 the transfer function between lateral offset with the preceding vehicle, y_L, and steering input, δ, is given by

$$\frac{y_L(s)}{\delta(s)} = \frac{-286.7s^5 - 3292s^4 - 1.399 \cdot 10^4 s^3 - 2.501 \cdot 10^4 s^2 - 1.464 \cdot 10^4 s - 2.132 \cdot 10^{-13}}{s^7 + 15.33s^6 + 92.94s^5 + 254.4s^4 + 265.5s^3} \tag{3.40}$$

The controller design and relevant closed loop functions are shown in appendix A.3. The transfer function used to stabilize the closed loop is a simple negative feedback gain given by

$$K_{y_L} = -1 \tag{3.41}$$

As can be seen from the transfer function given in (3.40), the relative degree is 2 and thus the system suffers from the limitations posed by the bode sensitivity integral also known as the water-bed effect. This causes a peak above 0 dB line for the sensitivity function (A.3) and consequently the conservative string stability plot violates lateral string stability condition as shown in figure 3.27(a). Figure 3.27(b) plots the global sensitivity function which confirms the significant amplification in error which goes on increasing along the string length. The analysis of the global sensitivity function is undertaken in more detail in the following subsection.

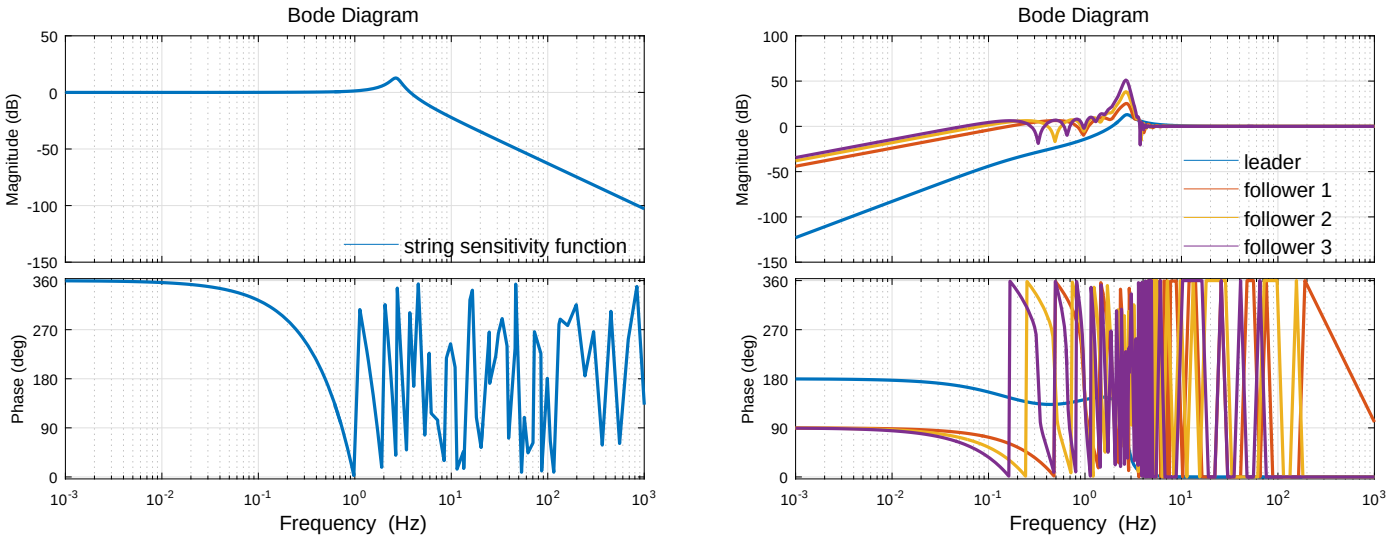

(a) Conservative lateral string stability condition

(b) Global sensitivity function

Figure 3.27: Lateral offset based lateral string stability

Simulation Results

In absence of feedforward, the designed controller is implemented to the system and simulated for the reference trajectory as described by figure 3.18. No limitations on steer input at wheels and steer rate are applied. As the figure 3.27 suggests, there are certain frequencies which are amplified violating the condition for conservative lateral string stability. For a constant longitudinal velocity of 15 m/s, the resultant simulation plots for trajectory and states are shown in figure 3.28.

The corresponding error profile is shown in figure 3.29 along with a closeup of the trajectory where the string instability is evident. The violation of the stability condition results in amplification of error implying string instability.

3.7.2 Lateral Velocity Based Feedback Controller

For design based on lateral velocity, the feedback controller in this case minimizes the difference between the reference state, i.e. lateral velocity from the preceding vehicle, and lateral velocity of the considered vehicle and produces the requisite control action. The transfer function between lateral velocity v and steering input δ is given by

$$\frac{v(s)}{\delta(s)} = \frac{45.44s^6 + 260s^5 + 482.8s^4 - 351s^3}{s^7 + 15.33s^6 + 92.94s^5 + 254.4s^4 + 265.5s^3} \tag{3.42}$$

The controller design and relevant closed loop functions are shown in appendix A.3. The transfer function used to stabilize the closed loop is a PI controller given by

$$K_v = \frac{-0.0008s - 0.1508}{s} \tag{3.43}$$

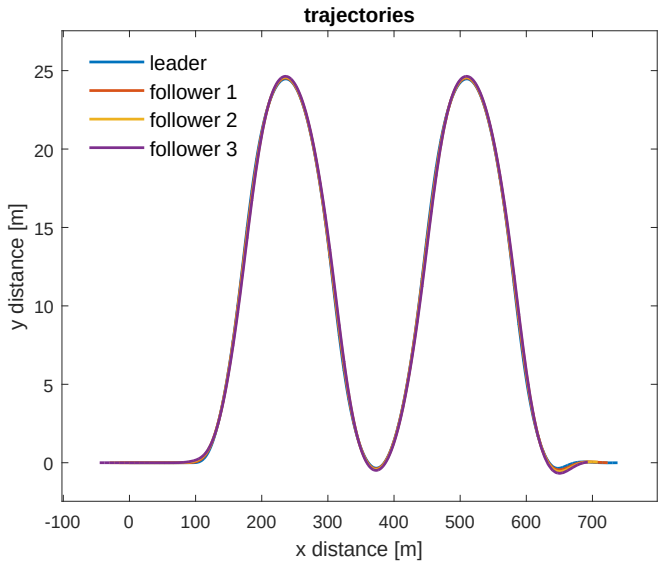

(a) Trajectories of vehicles in platoon

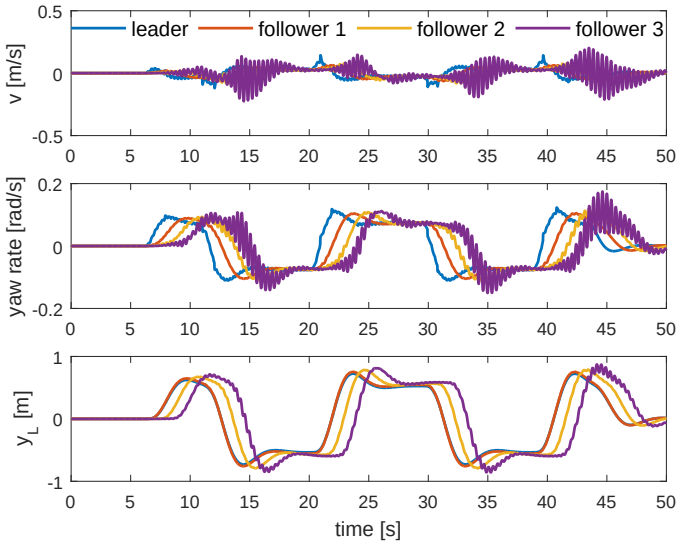

(b) States of vehicles in platoon

Figure 3.28: Lateral offset based controller simulation

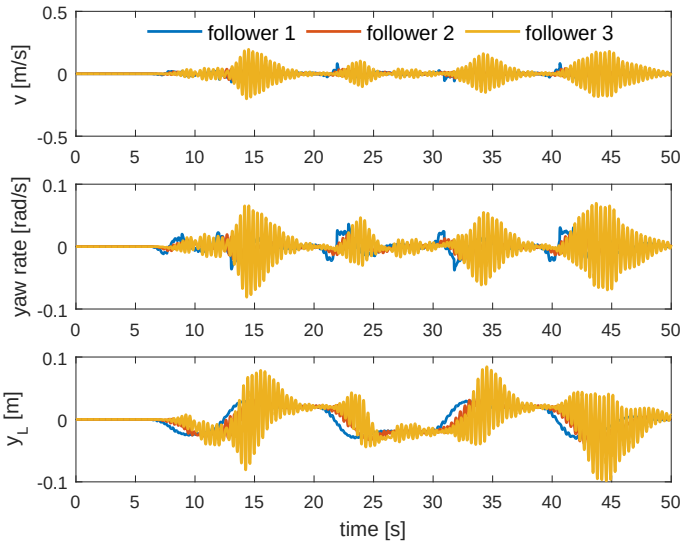

(a) Error profile for lateral offset based control design

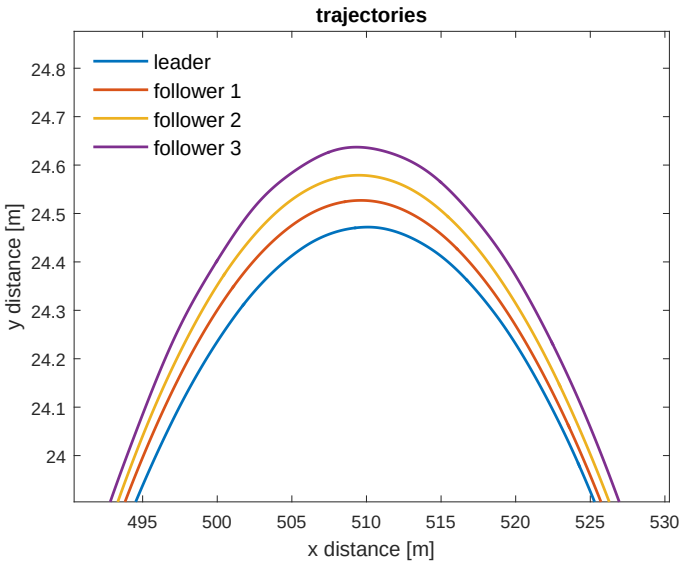

(b) Trajectory closeup indicating string unstable behavior

Figure 3.29: Error profile and string instability

Further analysis of the transfer function (3.42) shows that it is non-minimum phase which limits the performance characteristics for the controller. Another issue with such controllers is that the response moves in the opposite direction initially which makes it unfit for tracking applications.

It should also be noted that the transfer function has a relative degree of 1 as can be seen from (3.42) and hence, unlike the transfer function for lateral offset as discussed earlier, does not suffer from the water-bed effect. However, the bandwidth achieved to satisfy the condition for lateral string stability is very low and therefore not enough control action is generated for tracking application. The corresponding plots for lateral string sensitivity function is shown in figure 3.30.

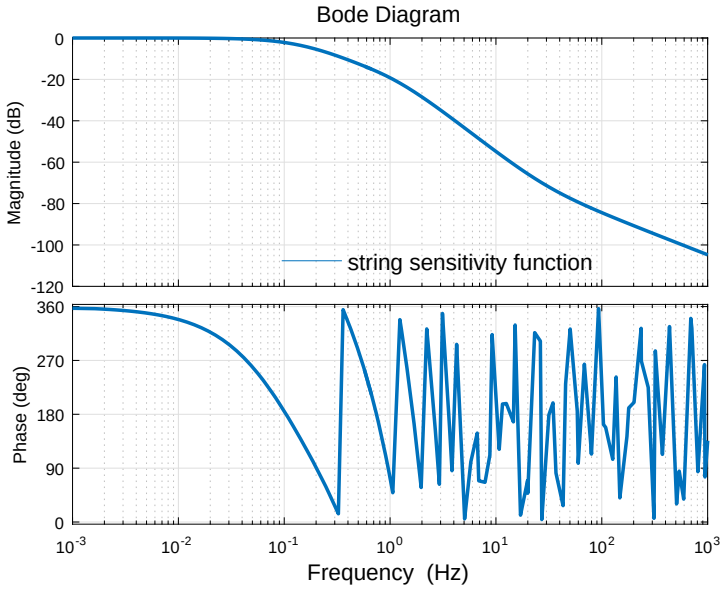

Figure 3.30: Velocity based lateral string stability

Simulation Results

Without feedforward, the designed controller based upon velocity is implemented to the system and simulated for the reference trajectory (figure 3.18). No limitations on steer input at wheels and steer rate are applied. As the figure 3.30 suggests, the condition for conservative lateral string stability is satisfied in the entire frequency range albeit with a considerably low bandwidth (approx. 0.08 Hz). For a constant longitudinal velocity of 15 m/s, the resultant simulation plots for trajectory and states are shown in figure 3.31 which depicts the inability of the controller to perform tracking.

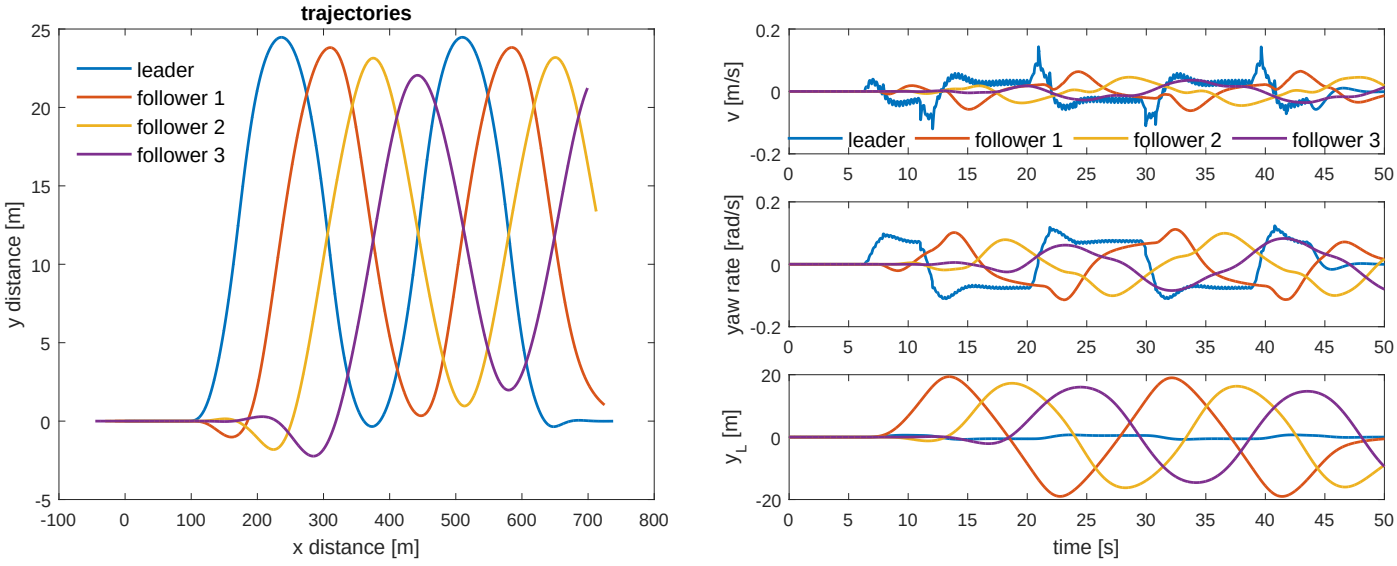

(a) Trajectories of vehicles in platoon

(b) States of vehicles in platoon

Figure 3.31: Velocity based controller simulation

The corresponding error profile is shown in figure 3.32. The non-minimum phase behavior of the system is also evident in the close-up view of the trajectory. It can be seen that the following vehicle moves in the opposite direction initially and consequently lags behind the leading vehicle enabling the error to build up.

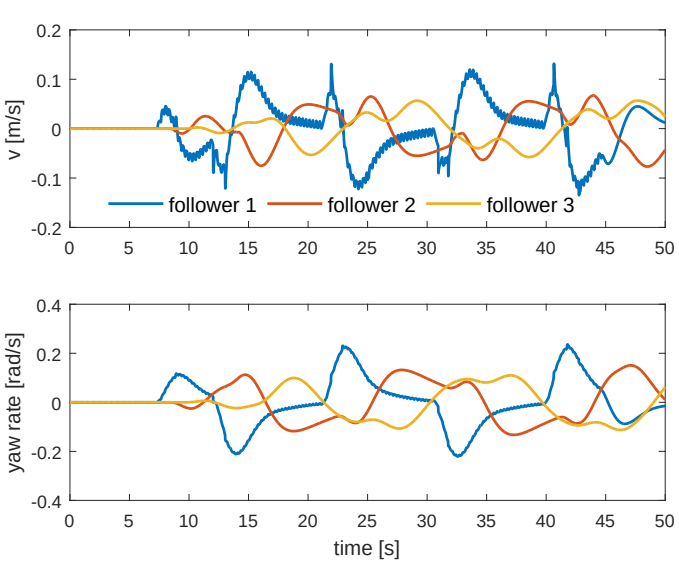

(a) Error profile for velocity based control design

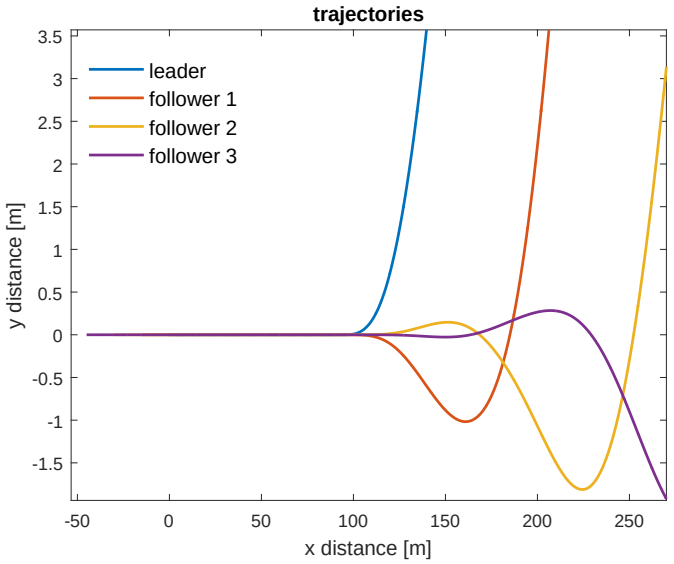

(b) Trajectory closeup showing non-minimum phase behavior

Figure 3.32: Error profile and instability

3.7.3 Yaw Rate Based Feedback Controller

The transfer function between yaw rate $\dot{\phi}$ and steering input δ is given by

$$\frac{\dot{\phi}(s)}{\delta(s)} = \frac{16.08s^6 + 186.1s^5 + 714.4s^4 + 976.3s^3}{s^7 + 15.33s^6 + 92.94s^5 + 254.4s^4 + 265.5s^3} \tag{3.44}$$

The Nyquist plot and relevant closed loop functions are shown in appendix A.3. The transfer function used to stabilize the closed loop is a PI controller given by

$$K_{\dot{\phi}} = \frac{s - 3.142}{s} \tag{3.45}$$

Like the transfer function between velocity and steering input, the yaw rate transfer function has a relative degree of 1 and hence does not suffer from the water-bed effect. Consequently a stabilizing controller based on yaw rate always satisfies the conditions (3.25) derived for lateral string stability. It is interesting to note that, given the transfer function has relative degree 1, a stabilizing controller yields string stable behavior for the lateral dynamics since the system does not suffer from water-bed effect.

The plots for lateral string sensitivity and global sensitivity function are shown in figure 3.33. As expected the lateral string stability condition is satisfied for all frequencies. The plot for global sensitivity function yields some interesting observations. The input frequency up to which error attenuation is possible decreases along the position in the string length. In addition, the peak in the global sensitivity function also increases down the string length. However, due to restrictions imposed by the lateral string stability condition, the rate of increase in peak value decreases and the peak value tends to an upper bound for a platoon of infinite length which provides the bounds for the expected error.

Simulation Results

Similar to the previous cases, the designed controller based upon yaw rate is implemented to the system and simulated for the reference trajectory. No limitations on steer input at wheels and steer

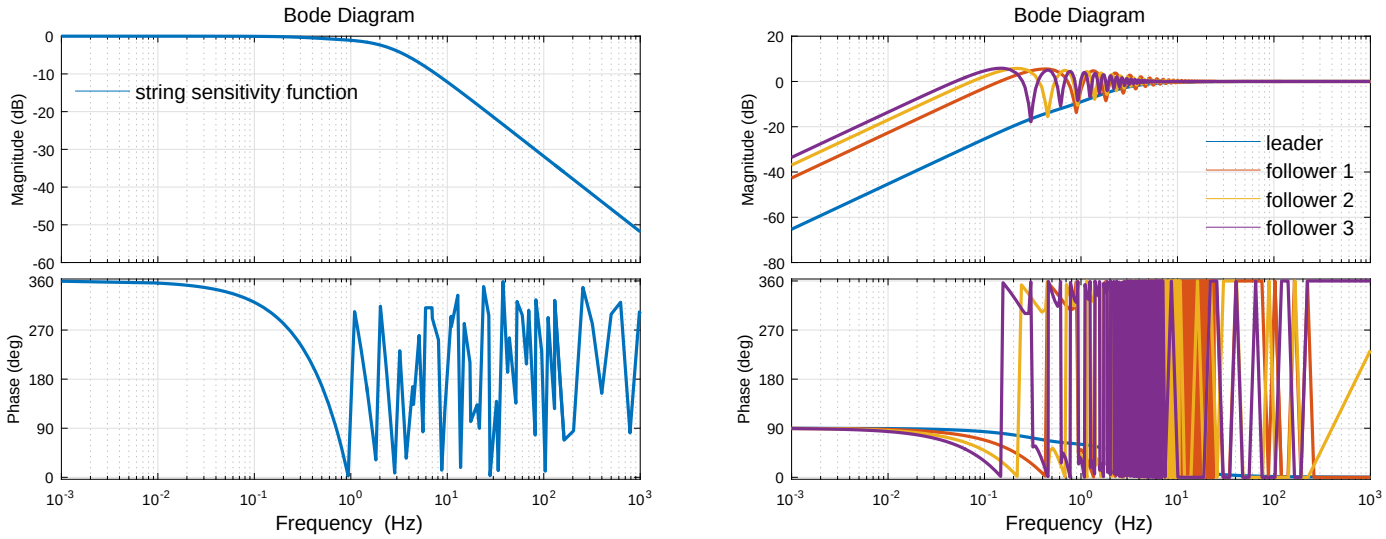

(a) Conservative lateral string stability condition

(b) Global sensitivity function

Figure 3.33: Yaw rate based lateral string stability

rate are applied. As the figure 3.33 suggests, the condition for conservative lateral string stability is satisfied in the entire frequency range. For a constant longitudinal velocity of 15 m/s, the resultant simulation plots for trajectory and states are shown in figure 3.34 which depicts the ability of the controller to perform tracking.

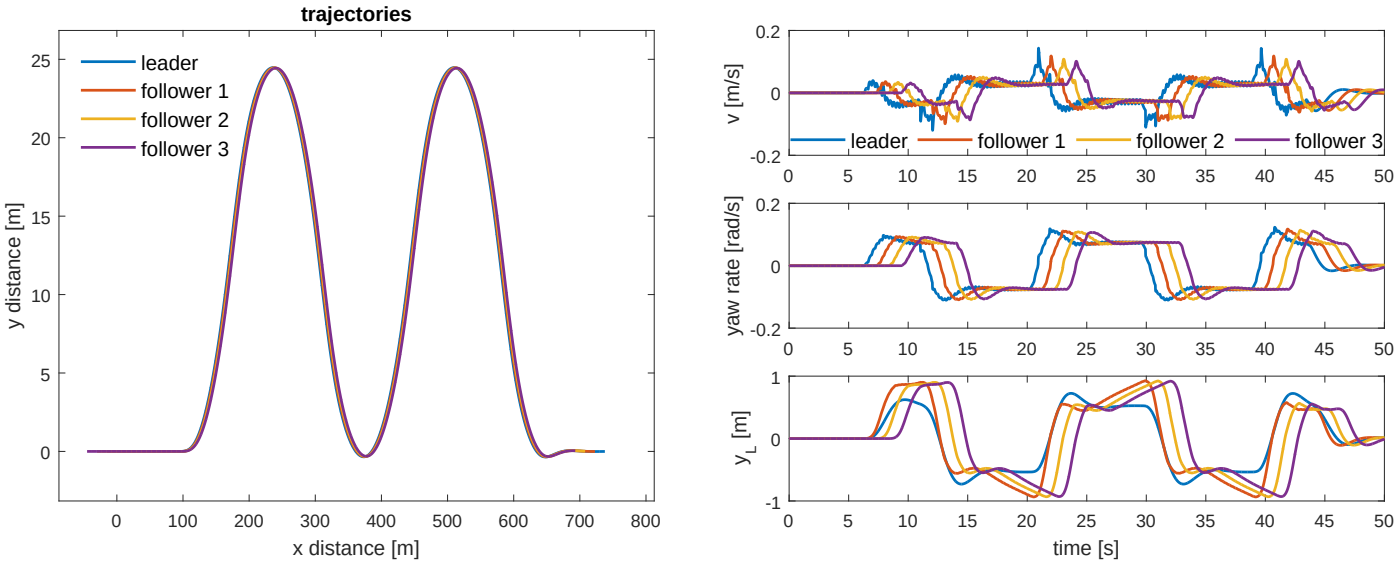

(a) Trajectories of vehicles in platoon

(b) States of vehicles in platoon

Figure 3.34: Yaw rate based controller simulation

The corresponding error profile is shown in figure 3.35. Since the controller satisfies the condition imposed for conservative lateral string stability, the subsequent error profiles are either the same or attenuated in comparison to the previous vehicle in the platoon. A close-up of the trajectory is shown to demonstrate the tracking performance of the controller design.

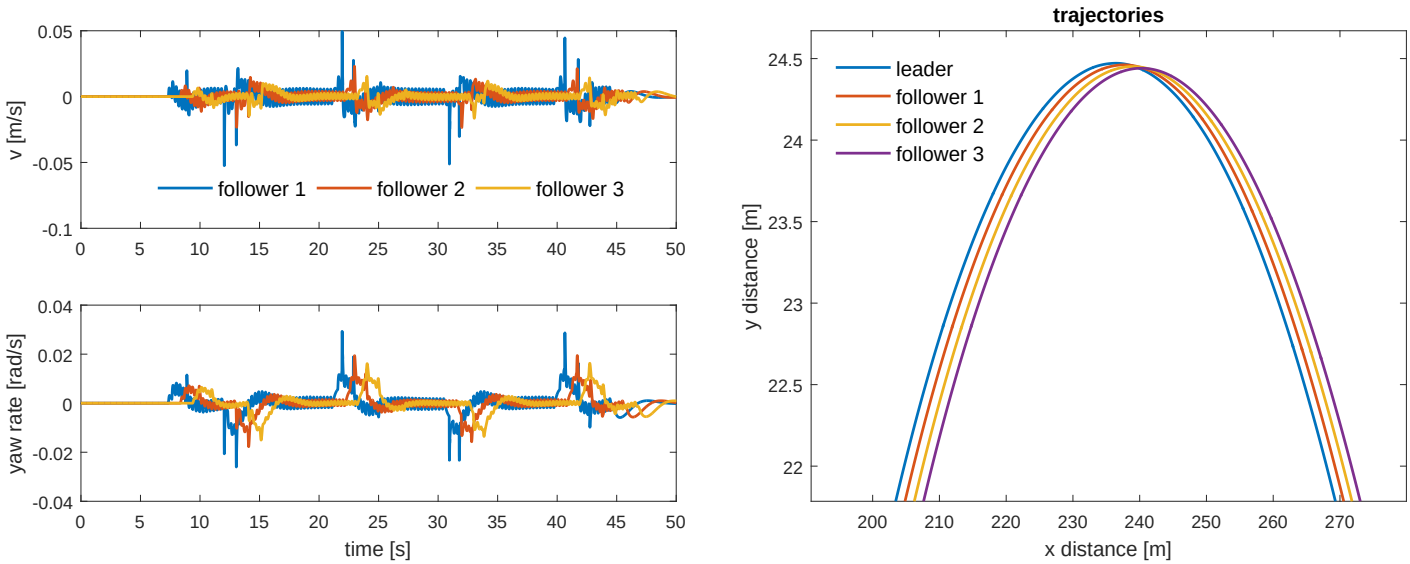

(a) Error profile for yaw rate based control design

(b) Trajectory closeup

Figure 3.35: Error profile and lateral string stability - yaw rate

3.7.4 Effect of Time Delay

The time delay, t_d, depends upon the longitudinal distance required between consecutive vehicles and also on the heading policy chosen. To understand its impact on error attenuation for lateral stability, the global sensitivity function is plotted in figure 3.36 for different values of delay. The plot shows dips, hence increase in error attenuation, at some frequencies **approximately** given by

$$f_{dip} = \frac{1/t_d}{i+1}$$

where f_{dip} represents the frequency at which these dips occur, t_d is the delay time between two consecutive vehicles and i is the i_{th} vehicle behind the platoon leader. This is merely and observation true for the given set of simulations and need to investigated further. It is also observed that as the time delay increases, the frequency at which the curve crossed 0 dB decreases and the peak error value increases albeit at a decreasing rate.

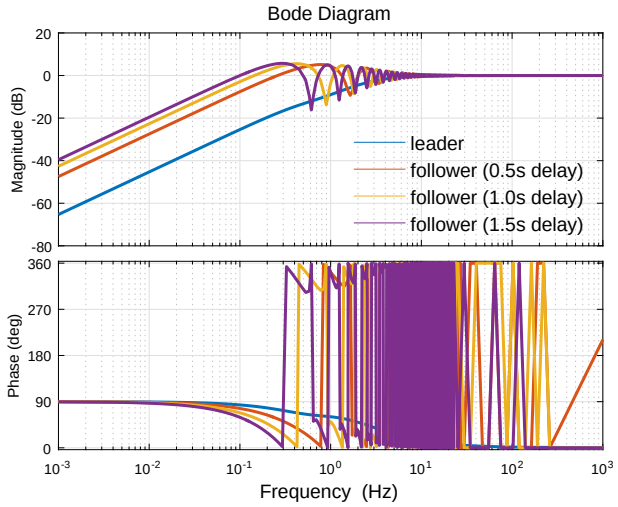

Figure 3.36: Effect of delay on global sensitivity function

3.7.5 Summary

In this section, controllers to achieve lateral string stability are designed without feedforward based upon the lateral string stability condition. The lateral offset based controller suffers from the water-bed effect and thus violates the condition for lateral string stability. The lateral velocity based controller is ineffective in tracking due to the non-minimum phase system, which puts restrictions on the bandwidth. A stabilizing yaw rate based controller satisfies the lateral string stability condition for all frequencies. From the global sensitivity plot (figure 3.33), it is observed that the global error increases as the number of vehicle increase and tends towards an upper bound. The plot also exhibits marked dips at certain frequencies as a result of the delay time. As the delay time increases, the peak error increases albeit at a decreasing rate and the effective frequency below which error attenuation occurs decreases.

3.8 Platooning Simulations: Including Feedforward

In a platoon of vehicles, similar to the longitudinal case, error amplification is an issue for the lateral direction along the string length. In section 3.6 conditions are derived to ensure error attenuation to enable lateral tracking of the leading vehicle in a platoon. Based upon the conditions derived, their effect on the design of a stabilizing control is investigated in section 3.7 and consequently controllers are designed. Simulations are performed with these controllers in absence of a feedforward to give insight into the string behavior for the homogeneous platoon.

In this section, feedforward combined with a feedback controller is simulated and analyzed. As discussed already, steering input at wheels δ is taken as the feedforward signal for all the simulations. The steering input from the preceding vehicle is delayed by constant desired headway in time.

3.8.1 Feedforward and Lateral Offset Based Feedback Controller

As demonstrated in section 3.7, a feedback controller based on lateral offset of the preceding vehicle does not satisfy the conditions for string stability resulting in certain input frequencies being amplified. The string instability is also evident in the simulation with feedforward. Figure 3.37 compares the error profiles and state plots of the vehicles in platoon. The amplification in error for follower 3 can be seen in figure 3.37(a) implying string instability. The corresponding trajectory is shown in figure 3.38 which shows amplification in tracking error around corners. It should be noted that the initial error arises due to the error in estimation of the reference for the lateral offset state. The error gets amplified along the string platoon and yields string instability despite feedforward.

3.8.2 Feedforward and Lateral Velocity Based Feedback Controller

As shown in section 3.7.2, a feedback controller based upon lateral velocity v is not suitable for tracking applications. Hence this case is not further explored.

3.8.3 Feedforward and Yaw Rate Based Feedback Controller

A yaw rate based stabilizing controller satisfies the conditions for lateral string stability and yields, in simulation, a tracking behavior along with feedforward control. The resultant plots of the simulation are shown in figures 3.39 and 3.40. As can be seen in figure 3.39(a), the error plots are at 0 value. However it will be shown in the subsequent section that yaw rate control alone is incapable of performing tracking in the presence of positional disturbances and requires use of sensors to locate the physical position of the vehicles in a platoon.

As expected, with feedforward the preceding vehicles track the leader of the platoon accurately.

The two simulations discussed above gives insight into the vehicle behavior in real scenarios where feedforward and feedback are used together to maintain a platoon formation. It was concluded in section 3.7 that feedback controllers based on lateral offset, as defined in this report, are

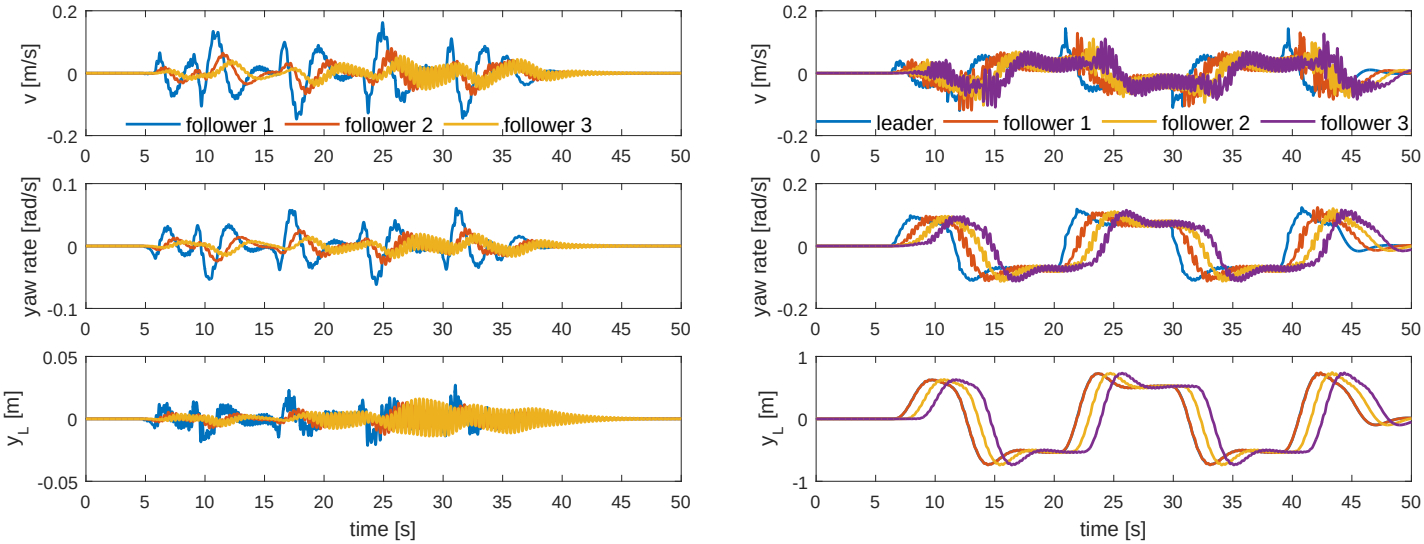

(a) Error plots

(b) State plots

Figure 3.37: Feedforward with lateral offset based controller design

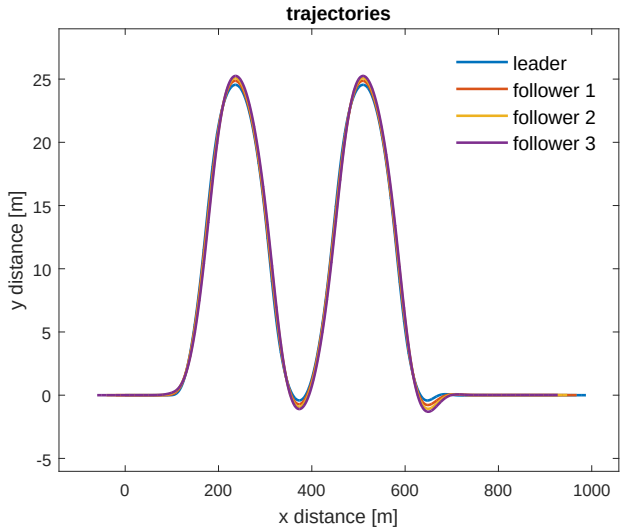

Figure 3.38: Trajectory plot - feedforward with lateral offset control

not string stable in the entire frequency range. This behavior is also present when combined with feedforward as clearly visible in error plots in figure 3.37(a). However a feedback controller based on yaw rate is shown to be string stable in combination with feedforward as demonstrated by error plots in figure 3.39(a). This makes feedback controller based on yaw rate suitable for platooning purpose. However, as discussed in section 3.7, the error with respect to the platoon leader increases albeit at a decreasing rate for vehicles upstream which is undesirable. Moreover, a yaw rate controller is incapable of detecting errors in position which would be explained in the next section.

3.8.4 Initial Condition Offset

A very common type of perturbation found in most systems is an initial condition offset. The lateral string stable controller is based upon yaw rate and hence any offset in position or orientation is not detected by the controller. To demonstrate this effect, a simulation is performed with small initial offset for the following vehicles in the platoon. The result is plotted in figure 3.41. Despite a big error in tracking as seen in the trajectory plot 3.41(a), the vehicle states do not detect it. The states

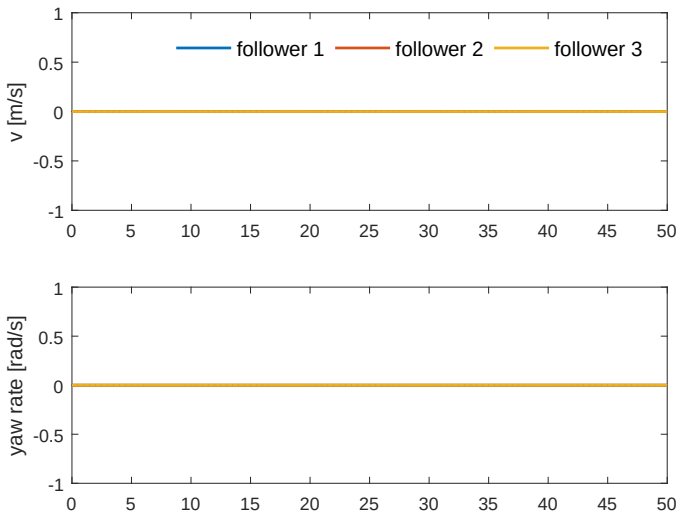

(a) Error plot - feedforward with yaw rate control

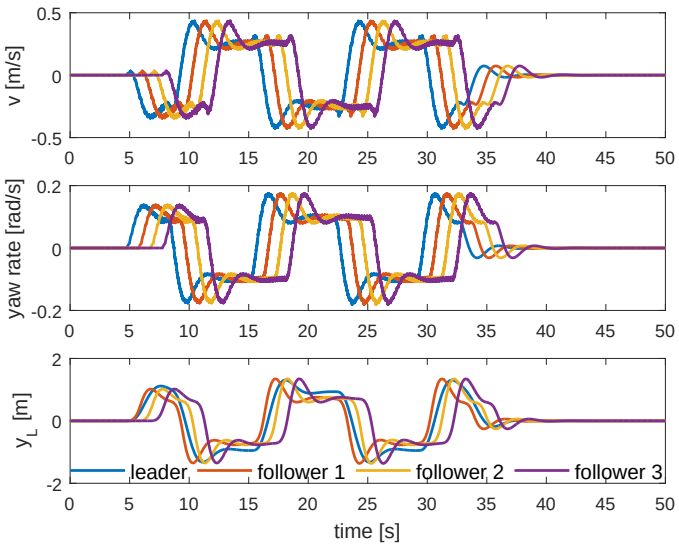

(b) States plot - feedforward with yaw rate control

Figure 3.39: Feedforward with yaw rate based controller design

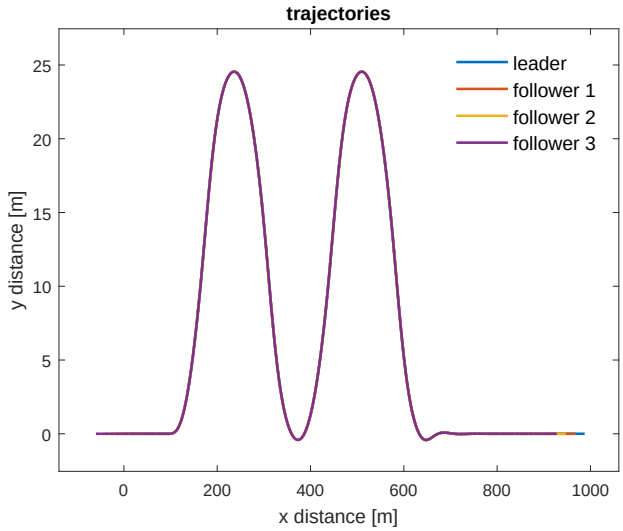

Figure 3.40: Trajectory plot - feedforward with yaw rate control

are identical for yaw rate and velocity.

This simulation demonstrates the importance of including sensor based controller design to achieve a robust lateral control. However due to water-bed effect it becomes essential to explore methods and techniques to utilize the information available over communication links that ensures lateral string stability using sensors such as two vehicle look-ahead control scheme, where the system interacts with preceding two vehicles, or communicate with the leader of the platoon.

3.8.5 Summary

In this phase, feedback controller based upon lateral offset and yaw rate designed in previous phase are combined with feedforward and simulated. The string instability is observed for lateral offset controller while the feedback controller based on yaw rate shows string stability. However for initial condition offset, the error is positions goes undetected by the yaw rate controller potentially result-

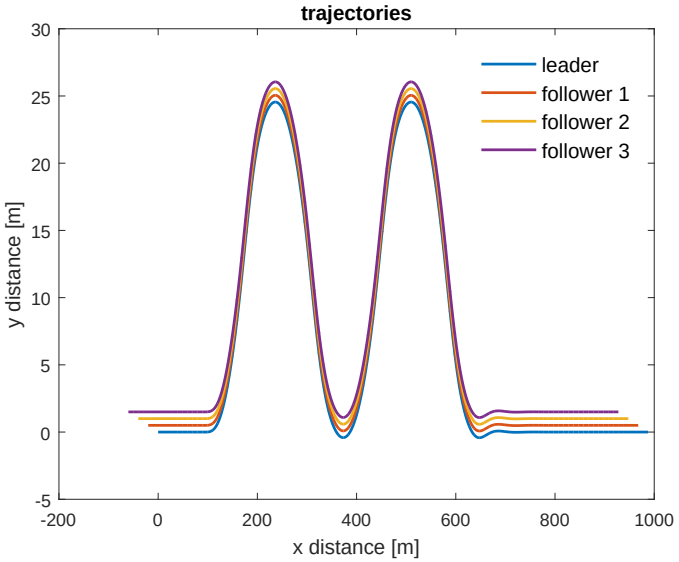

(a) Trajectory - initial condition offset

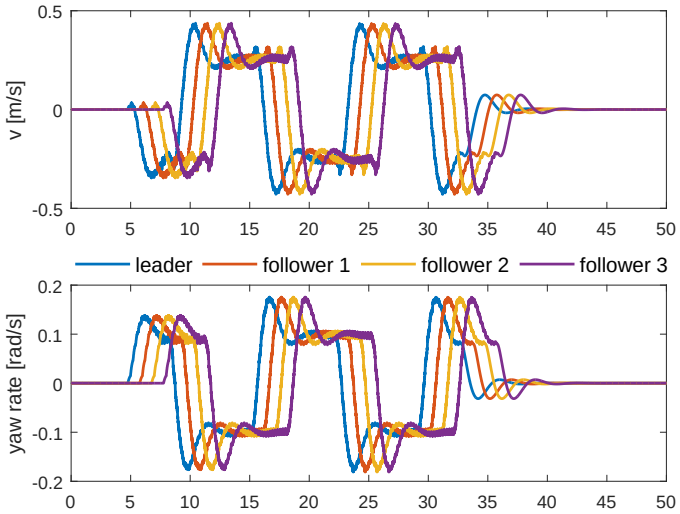

(b) State plots - initial condition offset

Figure 3.41: Effect of error in position in a vehicle platoon for yaw rate based control

ing in poor tracking. This necessitates the inclusion of sensor information (e.g. lateral offset y_L) to achieve robust tracking behavior in view of such disturbances.

3.9 Conclusions and Recommendations

3.9.1 Conclusions

The frequency domain analysis of lateral string stability yields some interesting conclusions which are listed below

1. For a perfect feedforward only marginal stability can be achieved implying the system is not robust to uncertainties. In such a case an accurate plant model is of utmost importance.

$$|SS_i| = \left|\frac{e_i}{e_{i-1}}\right| = |D| = 1, \qquad \forall\omega \ \ \& \ \ i > 1$$

2. In absence of feedforward, the frequency domain condition for lateral string stability without feedforward is given by

$$|SS_i| = \left|\frac{e_i}{e_{i-1}}\right| = |SGKD| \leq 1, \qquad \forall\omega \ \ \& \ \ i > 1$$

   The condition poses restrictions on the amplification of **local** error along a vehicle string. However it fails to give sufficient information on the **global** error with respect to initial reference trajectory. This makes the analysis of said global error important for tracking applications.

3. In absence of feedforward, the error relation between global error, the error with respect to initial reference for i_{th} vehicle in a platoon, and initial reference trajectory is given by

$$\hat{SS}_{i,g} = 1 - (SGKD)^i, \qquad \forall\omega \ \ \& \ \ i > 1$$

   The peak value of the global sensitivity function, $|\hat{SS}_{i,g}|_{max}$ increases along the vehicle string but the relative increase is bounded due to the lateral string stability condition. It should also be noted that the threshold frequency below which error attenuation is possible for the last vehicle in the platoon goes on decreasing as the number of vehicles in the platoon increases but $|\hat{SS}_{i,g}|_{max}$ also tends to saturate to an upper bound. The objective in such a case would be to minimize this value by means of a control algorithm.

4. Delay affects the performance of the tracking controller with respect to the original reference trajectory. Increase in delay time causes larger global error and decrease in effective frequency for error attenuation for vehicles along the platoon string.

5. Given the conditions derived for lateral string stability, feedback based upon lateral offset of the preceding vehicle under the assumptions of constant longitudinal velocity cannot achieve lateral string stability. This is due to the water-bed effect. However effect of additional sensor to measure the lateral offset of the following vehicle for lateral stability needs to be explored [9] for lateral case.

6. The existence of the so called heading policy, H, in case of longitudinal string stability is not present for the lateral case.

7. Given the conditions derived for lateral string stability, feedback based on lateral velocity control often leads to poor tracking because the plant is non-minimum phase which greatly limits the bandwidth and hence performance of the controller.

8. Given the conditions derived for lateral string stability, a stabilizing feedback controller based on yaw rate is sufficient to achieve lateral string stability because the relative degree of the transfer function between steering input and yaw rate is 1 and hence does not suffer from water-bed effect.

9. A feedback controller based only on yaw rate control is incapable of tracking laterally since it cannot detect changes/disturbances with respect to actual position of the vehicles in a platoon. Hence, inclusion of sensor capable of measuring position of vehicles in a platoon can be essential for tracking. In addition a smarter problem formulation or error definition may be explored which leads to satisfaction of tracking/vehicle following requirements along with yaw rate based feedback control.

10. The issue of initial condition offset of similar nature, as in lateral case, is not present for the longitudinal case since the definition of error in this case is based on actual difference in trajectory (in terms of difference in desired and actual inter-vehicular distance). Such a definition for lateral case could be the lateral offset with respect to the preceding vehicle y_L but as stated earlier such an arrangement suffers from water-bed effect.

11. Given the necessity to include sensor to cope with initial condition perturbations, it becomes essential to ensure string stability for the appended state y_L (lateral offset w.r.t. preceding vehicle). For this some possibilities that can be explored are communication with multiple vehicles, communication with the platoon leader and use of multiple sensors.

3.9.2 Recommendations

The analysis is based on bicycle model of the vehicle with a lot of assumptions that may not apply to real life conditions, for example, constant longitudinal velocity. Such assumptions restrict the scope of application for the designed controller and maybe a hindrance to the development of an autonomous vehicle. However inclusion of longitudinal velocity as a variable parameter makes the model nonlinear and difficult to deal with mathematically. This calls for use of nonlinear techniques and provides a direction for future research on the topic. In addition, the analysis takes into consideration interaction with only the preceding vehicle. However, as with the longitudinal case, information can be secured from multiple vehicles both in front and rear of the vehicle as well as from the platoon leader. A possible future work of this assignment could be the exploration of such communication permutations to ensure error attenuation over a wider range of frequencies.

Given the amount of existing research and interest in the topic from an economic standpoint, the future of autonomous vehicles is exciting as well as inviting.

Appendix A

A.1 Vehicle Parameters

The symbols used for the kinematic bicycle model of the tractor-trailer combination in Auto Docking is listed in table A.1.

Table A.1: Variables used for bicycle model

parameter	description	units
x_A	absolute x-coordinate of the center of the trailer rear axle w.r.t. fixed frame	m
y_A	absolute y-coordinate of the center of the trailer rear axle w.r.t. fixed frame	m
F	front axle of the tractor	-
B	tractor-trailer coupling point	-
D	center of the rear axle of the tractor	—
A	center of the rear axle of the trailer	—
a_1	distance between F and B	m
b_1	distance between B and D	m
b_2	distance between B and A	m
l	wheelbase of the tractor	m
β_1	orientation of the tractor w.r.t. fixed frame	rad
θ	articulation angle between tractor and trailer	rad
δ	steering input at wheel at front axle of the tractor	rad
u	constant longitudinal velocity	m/s

The parameters and corresponding values used for the dynamic bicycle model for the tractor-trailer combination used for vehicle platooning is listed in table A.2.

Table A.2: Parameters used for bicycle model

Parameter	Description	Value	Units
m_1	mass of tractor	7760	kg
m_2	mass of trailer	30102	kg
I_{zz1}	tractor moment of inertia about C.G. $4.42 \cdot 10^4$	kgm^2	
I_{zz2}	tractor moment of inertia about C.G.	$3.82 \cdot 10^5$	kgm^2
u	tractor longitudinal velocity	15	m/s
y_1	lateral motion of tractor C.G. w.r.t. body fixed frame	-	m
y_2	lateral motion of trailer C.G. w.r.t. body fixed frame	-	m
ϕ_1	heading angle - tractor	-	rad
ϕ_2	heading angle - trailer	-	rad
F_{yi}	lateral force generated at axle i	-	N
F_{hitch}	lateral force generated at hitching point	-	N
l_1	distance between tractor C.G. and tractor front axle	1.0160	m
l_2	distance between tractor C.G. and tractor rear axle	2.5840	m
l_3	distance between trailer C.G. and 1^{st} trailer rear axle	1.5438	m
l_4	distance between trailer C.G. and 2^{nd} trailer rear axle	2.7938	m
l_5	distance between trailer C.G. and 3^{rd} trailer rear axle	4.0438	m
l_6	distance between tractor C.G. and hitching point	2.1140	m
l_7	distance between trailer C.G. and hitching point	5.1062	m
C_1	cornering stiffness at tractor front axle	465276	N/rad
C_2	cornering stiffness at tractor rear axle	935136	N/rad
C_3	cornering stiffness at 1^{st} trailer rear axle	515700	N/rad
C_4	cornering stiffness at 2^{nd} trailer rear axle	515700	N/rad
C_5	cornering stiffness at 3^{rd} trailer rear axle	515700	N/rad
α_i	tire slip angle at axle i	-	rad
θ	articulation angle between tractor and trailer	-	rad
δ	steering input at the front wheels	-	rad

A.2 Design of Reference Shaping Filter K_c

In section 3.5.3, it is proposed to use the yaw information from the preceding vehicle to create a reference profile for the lateral offset y_L for the following vehicle to track. To rewrite (3.12)

$$y = \frac{d^2}{2\left(\frac{u}{\dot{\phi}}\right)} \tag{A.1}$$

Using the reference as described above, a simulation is performed based on the control scheme given in figure A.1. In the control scheme, steering input δ from the preceding vehicle denotes the feed-forward signal. The results of the simulation are plotted in figure A.2. The plot shows improved in terms of corner cutting behavior but on close inspection shows that during the first turn, the following vehicle first goes to the wrong side before correcting for it. This results due to the fact that the compensation is derived for steady state conditions. This implies that the compensation instantly goes to steady state value while the actual vehicle builds up to this value.

To minimize this effect, the steady state lateral offset estimate can be shaped using filter, K_c so that the compensation builds up to the required value. A second order transfer function is chosen

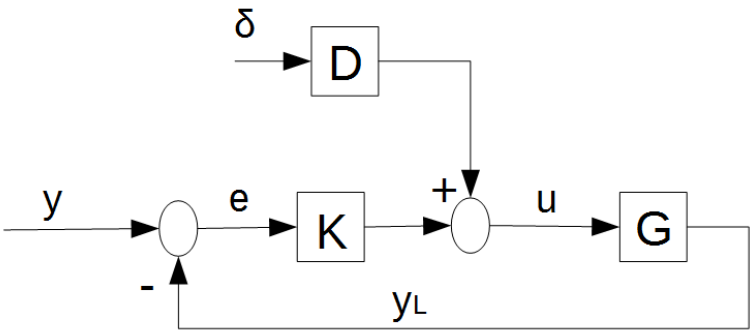

Figure A.1: Control scheme for feedback design based on lateral offset y_L

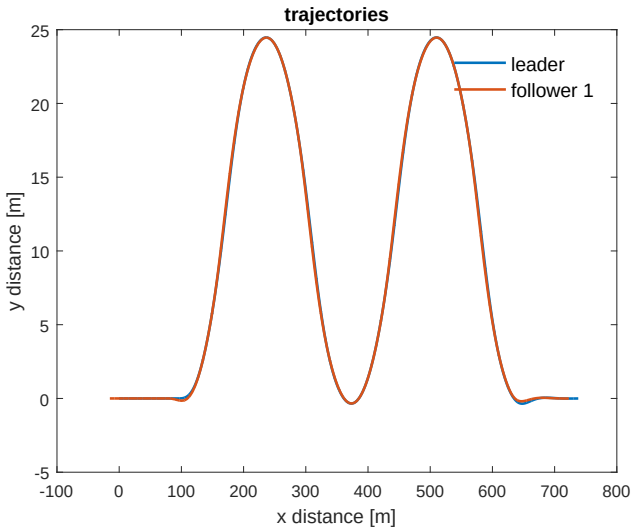

Figure A.2: Simulation with feedforward and feedback based on reference generated for lateral offset y for the following vehicle

for the filter K_c since motion systems generally behave like second order systems. The parameters are tuned specific to the vehicle model used for simulation and are given as

$$K_c = \frac{1}{0.5s^2 + s + 1} \tag{A.2}$$

The simulation result after addition of filter K_c, schematically shown in figure A.3, is shown in figure A.4. It can be seen that the vehicle no longer goes in the wrong direction initially which results in better tracking performance. The peak error is reduced to 0.01306 m.

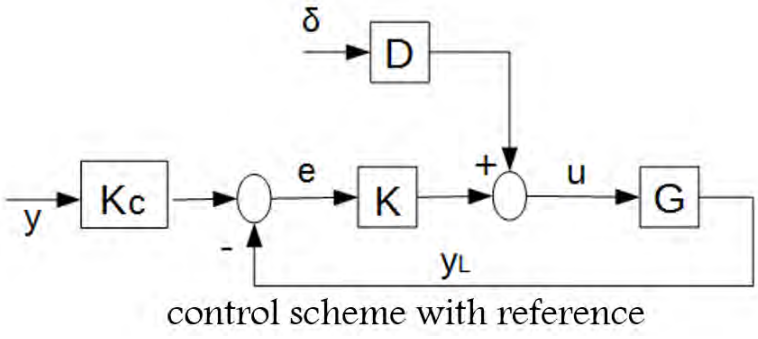

Figure A.3: Control scheme for feedback design based on lateral offset y_L and filter K_c

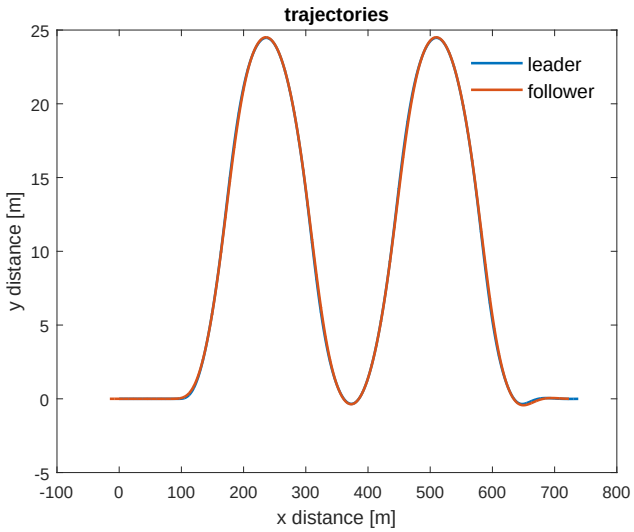

Figure A.4: Simulation with feedforward and feedback based on reference generated for lateral offset y for the following vehicle and filter K_c

A.3 Controller Design: Plots

A.3.1 Lateral Offset Based Feedback Controller

The corresponding transfer function for the lateral offset based feedback control is given as

$$\frac{y_L(s)}{\delta(s)} = \frac{-286.7s^5 - 3292s^4 - 1.399 \cdot 10^4 s^3 - 2.501 \cdot 10^4 s^2 - 1.464 \cdot 10^4 s - 2.132 \cdot 10^{-13}}{s^7 + 15.33s^6 + 92.94s^5 + 254.4s^4 + 265.5s^3} \tag{A.3}$$

and the stabilizing proportional controller K_{y_L} used for simulations is given by

$$K_{y_L} = -1 \tag{A.4}$$

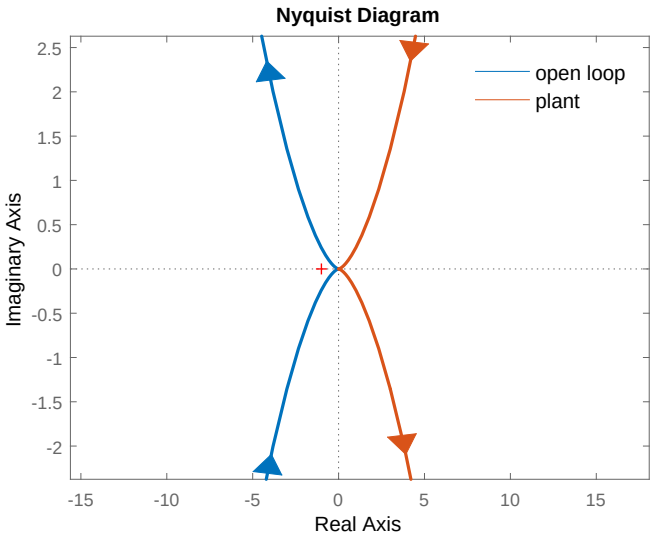

(a) Nyquist plot - lateral offset

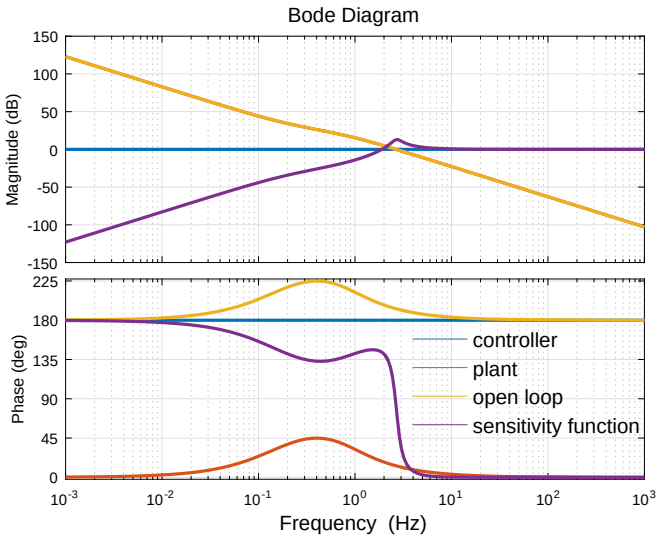

(b) Closed loop functions - lateral offset

Figure A.5: Lateral offset based controller design

A.3.2 Lateral Velocity Based Feedback Controller

The corresponding transfer function for the lateral velocity based feedback control is given as

$$\frac{v(s)}{\delta(s)} = \frac{45.44s^6 + 260s^5 + 482.8s^4 - 351s^3}{s^7 + 15.33s^6 + 92.94s^5 + 254.4s^4 + 265.5s^3} \tag{A.5}$$

and the stabilizing PI controller K_v used for simulations is given by

$$K_v = \frac{-0.0008s - 0.1508}{s} \tag{A.6}$$

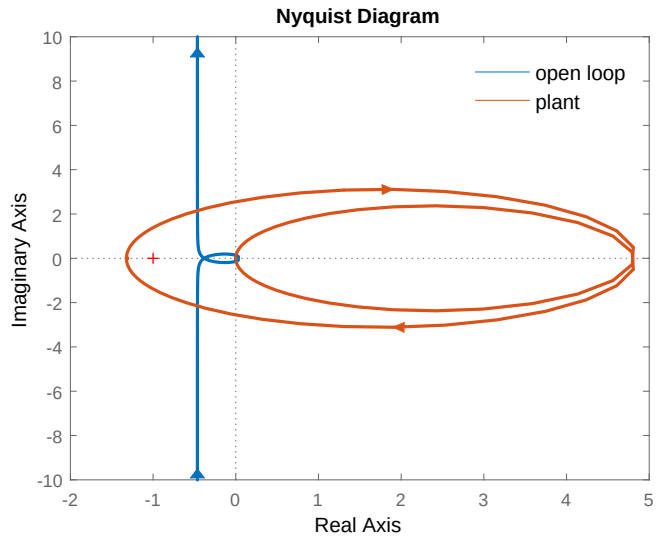

(a) Nyquist plot - velocity

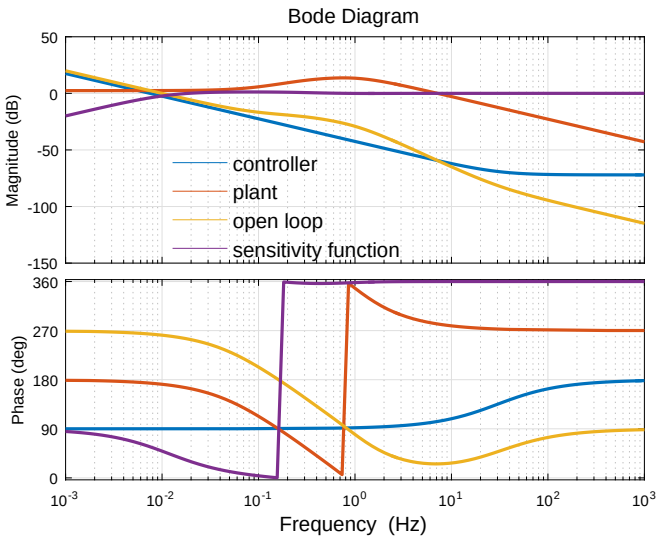

(b) Closed loop functions - lateral velocity

Figure A.6: Velocity based controller design

A.3.3 Yaw Rate Based Feedback Controller

The corresponding transfer function for the yaw rate based feedback control is given as

$$\frac{\dot{\phi}(s)}{\delta(s)} = \frac{16.08s^6 + 186.1s^5 + 714.4s^4 + 976.3s^3}{s^7 + 15.33s^6 + 92.94s^5 + 254.4s^4 + 265.5s^3} \tag{A.7}$$

and the stabilizing PI controller $K_{\dot{\phi}}$ used for simulations is given by

$$K_{\dot{\phi}} = \frac{s - 3.142}{s} \tag{A.8}$$

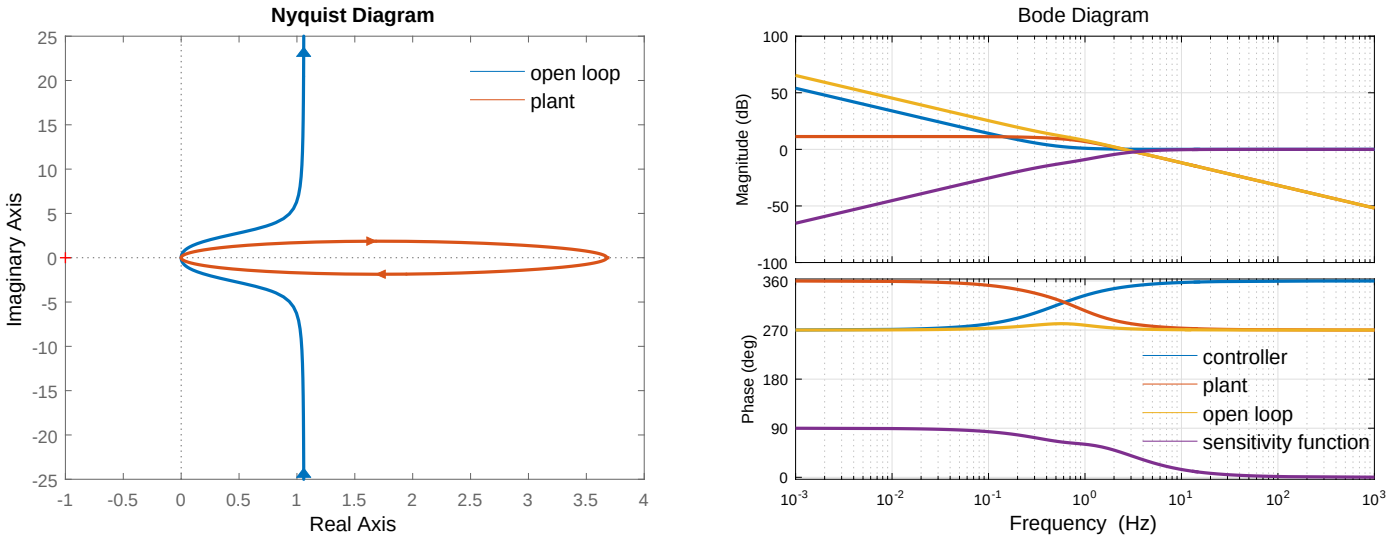

(a) Nyquist plot - yaw rate

(b) Closed loop functions - yaw rate

Figure A.7: Yaw rate based controller design

Bibliography

[1] Sai Krishna Yadlapalli, Swaroop Darbha, and K. R. Rajagopal. Information flow and its relation to stability of the motion of vehicles in a rigid formation. *IEEE TRANSACTIONS ON AUTOMATIC CONTROL, VOL. 51, NO. 8*, August.

[2] M. El-Gindy. Directional response of a tractor towing a semitrailer. *International Journal of Vehicle design*, 1989.

[3] A. D. George. Active lane keeping assist system (ALKAS). *SAI Technical Report, Eindhoven University of Technology*, September 2015.

[4] J. L. Naus Gerrit, P. A. Vugts Rene, Ploeg Jeroen, van de Molengraft Marinus J. G., and Steinbuch Maarten. String-stable CACC design and experimental validation: A frequency-domain approach. *IEEE TRANSACTIONS ON VEHICULAR TECHNOLOGY, VOL. 59, NO. 9*, November.

[5] T. Kabos. Design and implementation for a semi-trailer truck. *SAI Technical Report, Eindhoven University of Technology*, September 2015.

[6] Steffi Knorn and Richard H. Middleton. Two-dimensional analysis of string stability of nonlinear vehicle strings. *52nd IEEE Conference on Decision and Control*, December.

[7] F. A. B. Walter Niewoehoehner. Endangerment of pedestrians and bicyclists at intersections by right turning trucks. *Dekra Automobil GmbH*, September 2005.

[8] Lloyd E. Peppard. String stability of relative-motion PID vehicle control systems. *IEEE TRANSACTIONS ON AUTOMATIC CONTROL*, October.

[9] Jeroen Ploeg. *Analysis and Design of Controllers for Cooperative and Automated Driving*. 2014.

[10] T. Kabos, R. Dev Sharma, D. Tzempetzis, A. Khabbaz Saberi, P. Ramamurthy, and I. Konstantinou. Auto-docking proof-of-concept report. *SAI Technical Report, Eindhoven University of Technology*, September 2014.

[11] I. Surovtcev. Blind spot detection and passive lane change assist system. *SAI Technical Report, Eindhoven University of Technology*, September 2015.

[12] D. Swaroop and J. K. Hedrick. String stability of interconnected systems. *IEEE TRANSACTIONS ON AUTOMATIC CONTROL, VOL 41, NO 3*, March.

[13] Gerrit Naus, Rene Vugts, Jeroen Ploeg, Rene van de Molengraft, Maarten Steinbuch. Cooperative adaptive cruise control, design and experiments. *2010 American Control Conference Marriott Waterfront, Baltimore, MD, USA*, June 30-July 02.

[14] Jeroen Ploeg, Dipan P. Shukla, Nathan van de Wouw, and Henk Nijmeijer. Controller synthesis for string stability of vehicle platoons. *IEEE TRANSACTIONS ON INTELLIGENT TRANSPORTATION SYSTEMS, VOL. 15, NO. 2*, APRIL.

[15] Jeroen Ploeg, Nathan van de Wouw, and Henk Nijmeijer. $\mathscr{L}_p$ string stability of cascaded systems: Application to vehicle platooning. *IEEE TRANSACTIONS ON CONTROL SYSTEMS TECHNOLOGY, VOL. 22, NO. 2*, March.